Potential Sources of Salts from Water-Rock Interaction during Hydraulic Fracturing: An Experimental Study

Senior Thesis

Submitted in partial fulfillment of the requirements for the

Bachelor of Science Degree

At The Ohio State University

By

Michaela Wells

The Ohio State University

2015

Approved by

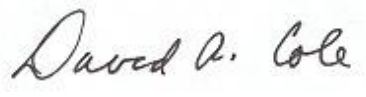

Dr. David A. Cole, Advisor

School of Earth Sciences

TABLE OF CONTENTS

Abstract

Studying the composition and chemistry of post-hydraulic fracturing flowback waters is important for understanding water-rock interaction in the subsurface and for how fluids injected into a well during the fracturing process can affect flowback water chemistry. A recent issue has risen involving the elevated concentrations of salts as total dissolved solids present in flowback waters. Scientists have been investigating whether these salts are being dissolved from the formation itself or if hydraulic fracturing fluids affect salt concentrations. This question was investigated by performing sequential leach experiments to determine how cation and anion concentrations dissolved into solution over time. Core and cuttings samples were obtained from southeastern Ohio. Core samples are from the Point Pleasant Formation and cuttings samples are from the Utica Formation. Various techniques were used to analyze samples including X-Ray diffraction (XRD) for bulk mineralogy, scanning electron microscopy (SEM) for mineral-textural and elemental data, and the use of PHREEQC Geochemical Modeling to determine saturation indices. The use of the SEM allowed for the assessment of the amount of barite and other minerals present after sequential leaching.

Acknowledgements

I have so much gratitude in my heart for anyone and everyone who has been a part of making my thesis a success as well as my college career. First and foremost, I would like to thank the School of Earth Sciences at The Ohio State University for finding me when I was young and in doubt and giving me a place to forever call my home not only academically but also for the wonderful people in the department that has been a part of my journey.

I would like to give the biggest thanks to Dr. Dave Cole for taking me under his wing and giving me the opportunity to be a part of the wonderful research group SEMCAL. I would like to thank him for his abundant amount of knowledge in last year and a half. I am forever grateful to Dr. Julie Sheets and Dr. Sue Welch for all of their time and effort put in to helping me prepare my samples and analyze my data and always being there the moment I need help or for the many, many emails and question that I have. Thank you both for your patience. Thanks goes to all of the SEMCAL members and friends who have helped in any way contribute to the work I have performed for this thesis.

I would like to thank all professors that have provided me with their knowledge in the classes I have taken that have equally contributed to my overall understanding of the Earth Sciences: Dr. Chin, Dr. Panero, Dr. Barton, Dr. Krissek, Dr. Olesik, Dr. Wilson, Dr. Cox, Dr. Judge, Dr. Kelly, Dr. Darrah, Dr. Millan, Dr. Royce, Dr. Sawyer, Dr. Durand, Dr. Carey and Dale Gnidovec. I wish to thank all of the graduate and undergraduate TA's for all labs and classes for all of the time and effort put in to my understanding in those classes. A big thanks to Dr. Royce for keeping me straight and figuring out the many problems that I seem to have as wells as all of the questions. Thank you for the patience!

A big thanks to any lab partners I have had in the major: Scott Hull, my Mineralogy and Petrology buddy always making working on labs fun and enduring. Same goes for my Apartment 9 roommates and friends at field camp: John Jones, Brendon Mock and Megan Mave. Thanks for all of the wonderful memories that will last a lifetime.

Thank you to my family. I would like to thank my mom, dad and sister for ALWAYS having faith in me even though there were times when we all weren't sure if I would make it this far. There aren't words to describe my love for my family and how that love gets me through every day. My grandparents on both sides who have always had faith in me, encouraged me and have prayed for me to accomplish all of my goals and watch me do great things. My aunts, uncles and cousins who have always kept interest in my personal and academic goals and have always been there for me even in distance. Thank you to my friends. Taylor Allen: This peach has been by my side since day 1 when I lost my BuckID in the stairwell of Houck House. We started in Chemical Engineering together and she was the reason I had found Earth Sciences. We switched to Earth Sciences together and she supports me in everything I do. She is always that bit of excitement and craziness that I need every day and in ES classes together with crazy jokes only we get and teachers who just don't understand. Bridgette Kelly: Now this girl has really been by my side since before day 1. We met on Facebook before Freshman year and she was my roommate. She is the sweetest, most loving, crazy girl I know and always has a way to cheer me up and to push on through all troubles. Maddie Duncan: This girl has been by my side since Freshman year. She is always there for me, gives words of support and wisdom and always cheers me up even in the worst of times. I would also like to thank all of the friends I have made in the School of Earth Sciences and I can honestly call all of them my family. Lastly, a big thanks to The Lord for always and forever being there, watching over me and guiding me in all endeavors and giving me the strength to always be the best person I can be. There are many other things I could say, but words can't do justice for how the heart feels...

1. Introduction

A growing concern has been identified involving the presence of salts as total dissolved solids in post-hydraulic fracturing flowback waters. Scientists have been investigating the characteristics of these dissolved solids from different gas shale systems to develop protocols to properly dispose of the flowback fluid under regulatory conditions. The quality of the flowback water can be dependent on many factors such as the chemistry associated with hydraulic fracturing fluids in contact with the formation, fluids in contact with formation water, the formation itself and the amount of time the fluid was retained in the well and the initial quality of the fluid used in the process (Vazquez et al. 2014).

The flowback water returns to the surface when pressure is released on the well. The majority of flowback returns within the first few days or weeks, while the remainder returns slowly over time as hydrocarbons are produced. During the first few days, the level of total dissolved solids rises very quickly with concentrations around 100 to 300 grams/liter after approximately 7-30 days (Stewart et al. 2015). The origin of dissolved solids, including the mixing with subsurface groundwater and dissolution of evaporates is still being studied (Stewart et al. 2015). When water-rock interactions take place, metals, salt ions and organic compounds can be released (Wilke, 2015).

This experimental study examines the extent to which water-soluble salts are released during water-rock interactions in sequential leach experiments. The purpose of this work is to investigate the mineralogical and chemical composition of core and cutting samples, and to conduct benchtop water-rock interaction experiments to determine the sources of dissolved solids in the flowback waters produced during hydraulic fracturing. The objective is to determine whether these dissolved constituents originate from the formation itself, the drilling muds or from hydraulic fracturing fluid used in the fracturing process?

2. Methods

2.1 Sample Description and Analytical Techniques

Several methods were used to prepare and analyze the cuttings and core samples of gas shale obtained from southeastern Ohio for this experiment. Two core samples were chosen because they were from the zone of interest for hydraulic fracturing and three cuttings samples were chosen to try and match core depths. However, it was later determined that core samples were from the Point Pleasant Formation and cuttings samples were from the overlying Utica Formation. Sample numbers are subsamples of the two core and three cuttings samples used in this experiment. Cuttings depths represent total distance within the hole, with some vertical component and some lateral component. Operators describe the depth to the turn (toward the lateral) as being around 7000 feet. Core and cuttings samples used in this experiment along with their corresponding depths, formations and leachates used are shown in Table 1 below:

Table 1: Samples and their corresponding depths, formations, leachates and type

Sample Number	Depth (ft)	Formation	Leachate Used	Type
M1	8549 ft	Point Pleasant	Water	Core
M2	8549 ft	Point Pleasant	Acid	Core
M3	8479 ft	Point Pleasant	Water	Core
M4	8479 ft	Point Pleasant	Acid	Core
M5	8470 ft-8500 ft	Utica	Water	Cuttings
M6	8500 ft-8530 ft	Utica	Water	Cuttings
M7	8530 ft-8560 ft	Utica	Water	Cuttings
M8	8470 ft-8500 ft	Utica	Acid	Cuttings
M9	8500 ft-8530 ft	Utica	Acid	Cuttings
M10	8530 ft-8560 ft	Utica	Acid	Cuttings

The supply of cuttings samples available from depths 8470 ft–8500 ft and 8530 ft–8560 ft was sufficient only to perform the sequential leach experiments. Cuttings from depth 8500 ft–8530 ft were used for mineralogical assessment via XRD and were not the same material used in the leach experiment. However, all cuttings came from the same formation, the Utica. As will be shown

below, a comparison of results from experiments using the core and cuttings does allow for a comparison between a clay-rich shale (the Utica) and a carbonate-rich shale (the Pt. Pleasant).

2.2 Sample preparation

Samples were first observed for physical characteristics, such as color and texture to note any differences related to sample depths. Then, approximately 1 gram of each sample was hand ground using a mortar and pestle. Gloves were worn during this process to avoid introducing contamination. Core samples were ground to approximately the same grain size (approximately silt to coarse clay sized) as cutting samples to avoid grain size bias. Mortar and pestle were thoroughly cleaned between each grinding session to avoid cross-contamination between samples.

2.3 X-Ray Diffraction

Core and cuttings samples were then prepared for XRD analysis to determine bulk mineralogical composition. A table of samples analyzed for XRD is presented in Table 2. All samples were loaded into a specified magazine slot and analyzed with a PANalytical X'Pert Pro X-ray diffractometer at the Subsurface Energy Materials Characterization and Analysis Laboratory (SEMCAL), School of Earth Sciences, The Ohio State University. This instrument is equipped with a high speed X'Celerator detector. Data were collected from 4 to 70 degrees 2-theta with a voltage of 45 keV and tube current of 40 mA (CuKα radiation). Sample scans were viewed and compared using PANalytical DataViewer software. The scans were then opened in PAnalytical HighScore Plus to be analyzed for bulk mineralogy. Data for all samples were corrected for background by applying a granularity of 19 and a bending factor of 0. Peak search was run using a minimum significance of 1.00, a minimum tip width of 0.10, a maximum tip width of 1.00 and a peak base width of 2.00. The method applied used a minimum 2nd derivative. Scans were analyzed with the pattern matching algorithm in HighScore Plus, using the PDF 4+ mineral database. Minerals relevant to the samples

were accepted as candidates and non-relevant minerals were rejected. Each candidate accepted was analyzed for pattern lines to ensure that the highest intensity lines were matched, leading to confidence in the mineral selected.

Table 2: XRD samples and their corresponding depths, formations and type

Samples used for XRD Analysis		
Depth (ft)	**Formation**	**Type**
8549 ft	Point Pleasant	Core
8479 ft	Point Pleasant	Core
8410 ft-8440 ft	Utica	Cuttings
8500 ft-8530 ft	Utica	Cuttings
8680 ft-8710 ft	Utica	Cuttings

2.4 Sequential Leach Experiments

In order to determine the readily soluble salt content of the solid phase, samples of the core and cuttings powders were subjected to a series of sequential leach experiments at room temperature and ambient pressure. Temperature and pressure conditions typical in the complex subsurface were not replicated in order to keep temperature and pressure a constant for this experiment. It is assumed that room temperature did not fluctuate more than a few degrees during the course of this experiment. Each sample was divided into two subsamples, weighing approximately 0.5g, and placed into a 50mL Falcon tube. All samples were weighed on a Mettler Toledo pan balance. Subsample weights are listed in Table 3A in Appendix A. One set of subsamples (M1, M3, M5, M6, M7) was leached in 50mL of distilled Mili-Q water. The second set of subsamples M2, M4, M8, M9 and M10 was reacted in 50 ml Mili-Q water with 0.5mL of 0.1M HCl (~ 1 mM HCl). As will be seen in the results, too much acid was inadvertently added to all samples for the fourth leach either by setting the automatic pipette incorrectly or by using the wrong bottle of acid. All samples were thoroughly mixed at the start of the experiment. Two experimental blanks were prepared using the same

distilled Milli-Q water plus acid to determine if salts or trace metals were present in the water, acid, or leached from the Falcon tubes.

All solid phase samples were leached sequentially 4 times, following the same fluid addition procedures for each set-up. The supernatant fluid was removed with a transfer pipette and solutions were filtered with a 0.45 micron pore size syringe filter. Not all of the supernatant fluid was removed during this process to avoid disturbing the powdered rock sample in order to keep the water-rock ratio fairly consistent. The time for each leach experiment was increased for subsequent leaches to simulate increased water-rock interaction time in the subsurface. Leach 1 was allowed to sit for 1 day and then fluid was removed. Leach 2 lasted 2 days, leach 3 lasted two weeks, and leach 4 was sampled after three weeks. After Leach 1, the Falcon tubes were reweighed before continuing to the set-up of Leach 2, to ensure minimal solid phase sample loss during the removal of fluid, and also to ensure that the fluid-rock ratio would still be approximately the same. After the supernatant fluid was removed from Leach 4, the solid phase samples were allowed to air dry before analysis using the SEM. Fluid samples were analyzed for select major and trace elements using an Inductively Coupled Plasma Optical Emission Spectrometer (ICP-OES). Anion concentrations were measured using a Dionex Ion Chromatograph using the methods of Welch et al. (1996).

2.5 Scanning Electron Microscopy (SEM) and Energy Dispersive X-Ray Spectrometry (EDXS)

The core and cuttings samples from the final leach experiment were prepared for analysis with the FEI Quanta 250 Field Emission SEM. A small fraction of the reacted powder was adhered to an aluminum stub with carbon tape. Loose material was tapped off the stubs before coating with Au/Pd with a Denton Desk V precious metal sputter coater to prevent charging.

Images were acquired using a backscattered electrons BSE detector and a secondary electron detector (Everhart-Thornley). Images were acquired using an accelerating voltage of 15keV, a

working distance of ~13 mm and a spot size of 4.0. Spot analyses were taken of regions of interest using a Bruker Xflash Energy Dispersive X-Ray Spectrometer. The energies of characteristic X-rays were used to determine the elemental compositions of minerals subjected to the spot analysis.

2.6 PHREEQC Geochemical Modeling

Geochemical modeling was used to determine saturation indices of selected phases using PHREEQC version 3.1.7-9213. This version can be downloaded from the United States Geological Survey website: http://wwwbrr.cr.usgs.gov/projects/GWC_coupled/phreeqc/ . Solution alkalinity was estimated for each sample from the charge balance between measured anions and cations.

3. Results

3.1 X-ray diffraction of cuttings and core samples prior to sequential leaching

XRD analysis was used to determine bulk mineralogy of the core and cuttings samples used in the leach experiments. Understanding the initial mineral composition is necessary for assessing sample textures and mineralogy *after* the leach experiments. Core and cuttings samples analyzed on XRD along with their corresponding depths and formations are shown in Table 2.

It must be kept in mind that core and cuttings samples represent rock from different depths, and more importantly different formations. This difference is reflected in the XRD data (Figure 1). Core samples represent a true vertical depth, while cuttings samples represent a *total* depth from the borehole which includes vertical as well as lateral depth when drilling took a turn in the process. XRD individual raw data scans are in presented in Appendix A. Based on log data and the XRD results, the core samples represent rock material from the Point Pleasant, while cuttings represent material from the Utica.

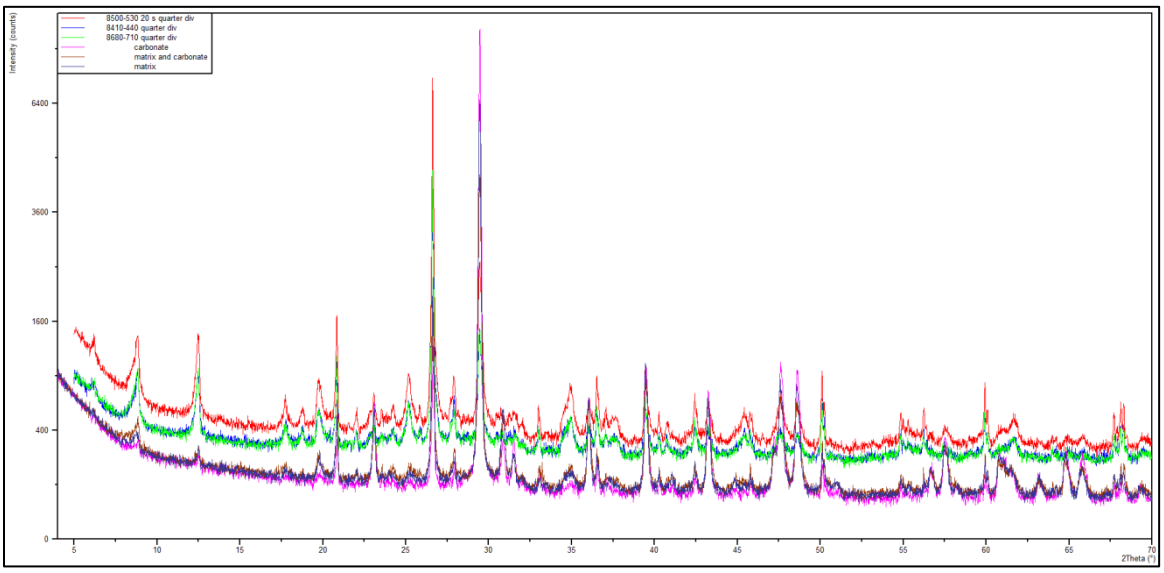

Figure 1: Combined core and cuttings raw data. Purple corresponds to core from depth 8479 ft (predominantly fine-grained matrix) in the Point Pleasant Formation, pink -core from depth 8479 ft (predominantly carbonate), brown- core from depth 8549ft (carbonate and matrix). Blue corresponds to cuttings from depth 8410 ft-8440 ft from the Utica Formation, red- cuttings from depth 8500 ft-8530 ft, green- cuttings from depth 8680 ft-8710 ft.

3.1.1 Cuttings samples

The XRD scan for cuttings sample at a depth of 8410 ft–8440 ft shows a clay-rich mineralogy (Figure 2). This scan includes results of the peak matching routine in the HighScore Plus analytical platform. Illite/muscovite are identified based on the 10-angstrom d-spacing peak at 9.01 degrees 2-theta. Calcite and dolomite are identified based on the 100 relative intensity lines at 29.43 and 30.98 degrees 2-theta, respectively, as well as the presence of most expected peaks over the entire 2-theta range of the scan (5-70 degrees 2-theta). Pyrite is evident based on the 1.63-angstrom d-spacing peak at 56.34 degrees 2-theta. The highest intensity (major) peak for albite is identified at 28.0 degrees 2-theta (d-spacing 3.19 angstroms). The 14-angstrom (001) peak for chlorite (pattern matched to clinochlore) is also present, as is its corresponding 7-angstrom (002) peak around areas of 4.0 and 12.0 degrees 2-theta. Strontianite is identified based on the peak at 25.86 degrees 2-theta (the 100 relative intensity line), but its identification is tenuous based on peak overlap with clinochlore. The 100 relative intensity line for barite (not shown) can be identified based on a 3.45-angstrom d-spacing (25.86 degrees 2-theta) that may overlap with strontianite.

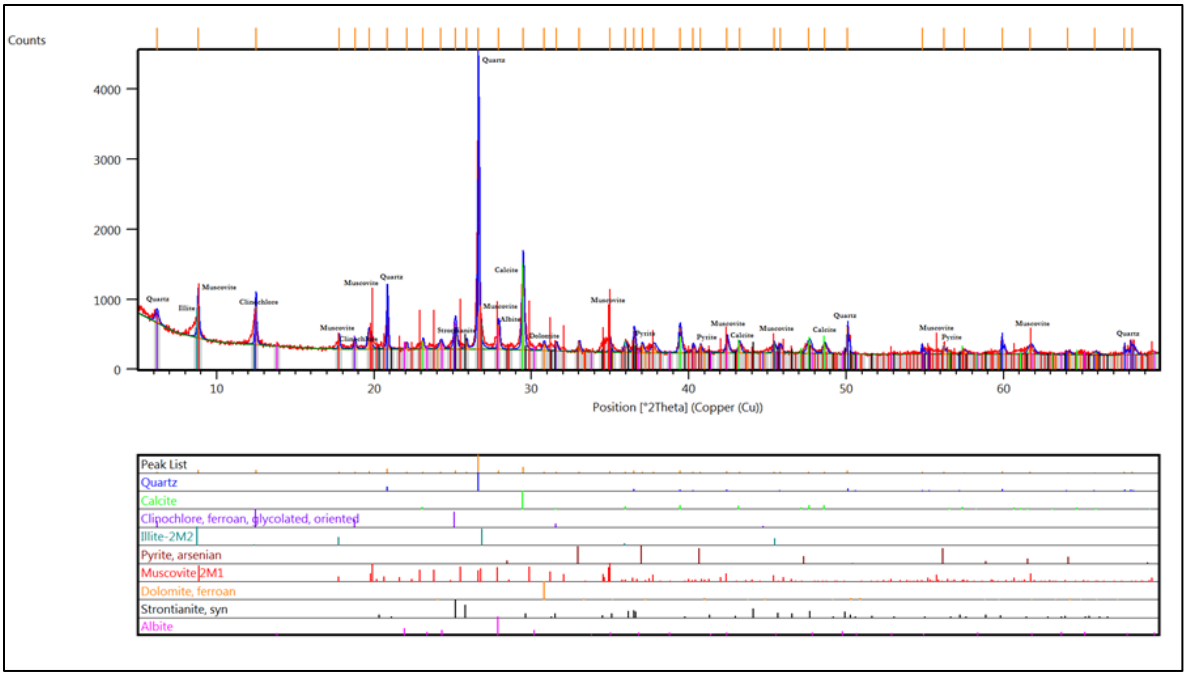

Figure 2: XRD scan for cuttings depth 8410 ft–8440 ft (one-quarter divergence slit), showing minerals identified

The cuttings sample from depth 8500 ft–8530 ft also has a clay-dominated mineralogy (Figure 3). Much like cuttings depth 8410 ft–8440 ft, illite, muscovite, and chlorite compose the phyllosilicates. Other major minerals include calcite, dolomite, and quartz, with minor pyrite and albite. Strontianite is tentatively identified based on its major peak at the 25.86 degrees 2-theta position but again, this overlaps with clinochlore.

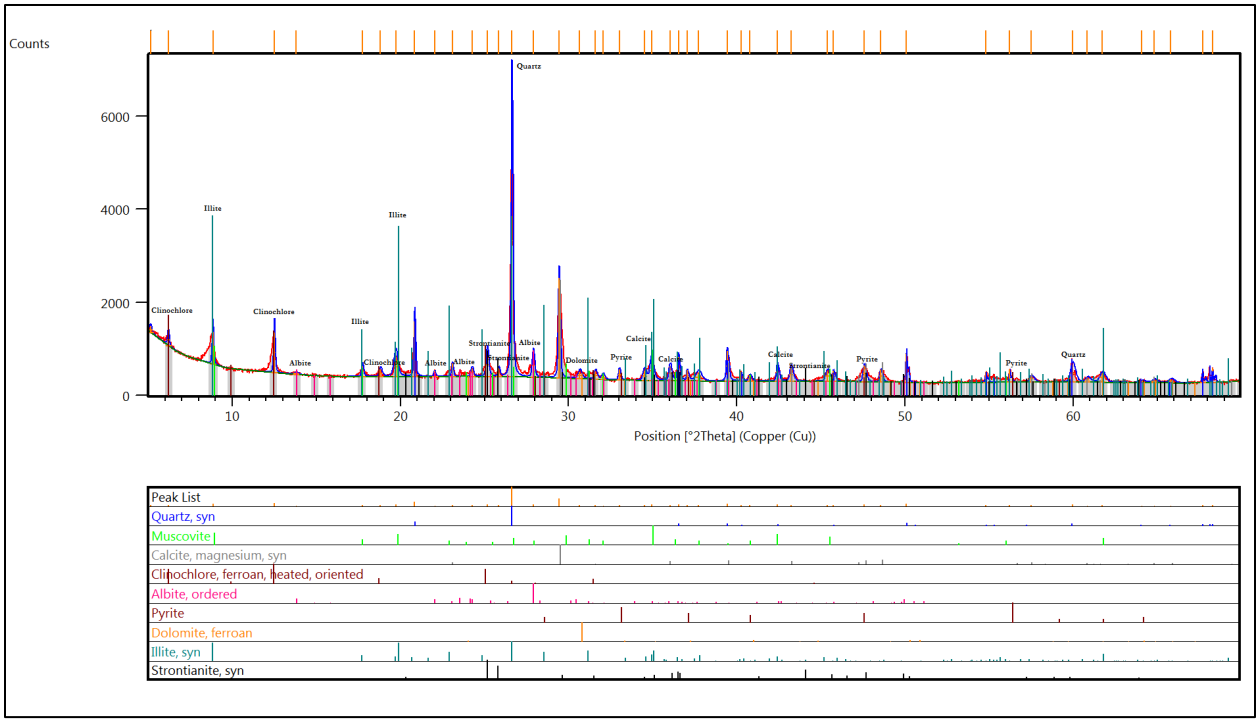

Figure 3: XRD scan for cuttings depth 8500 ft–8530 ft (20s count time; one-quarter divergence slit)

The cuttings sample from depth 8680 ft–8710 ft has a clay dominated mineralogy much like the previous cuttings depths shown (Figure 4). Calcite, dolomite and quartz with minor amounts of pyrite and albite are present. As with the sample from depth 8500–8530 ft, strontianite is defined by its high intensity peak at around 25.86 degrees 2-theta but this shows overlap with clinochlore.

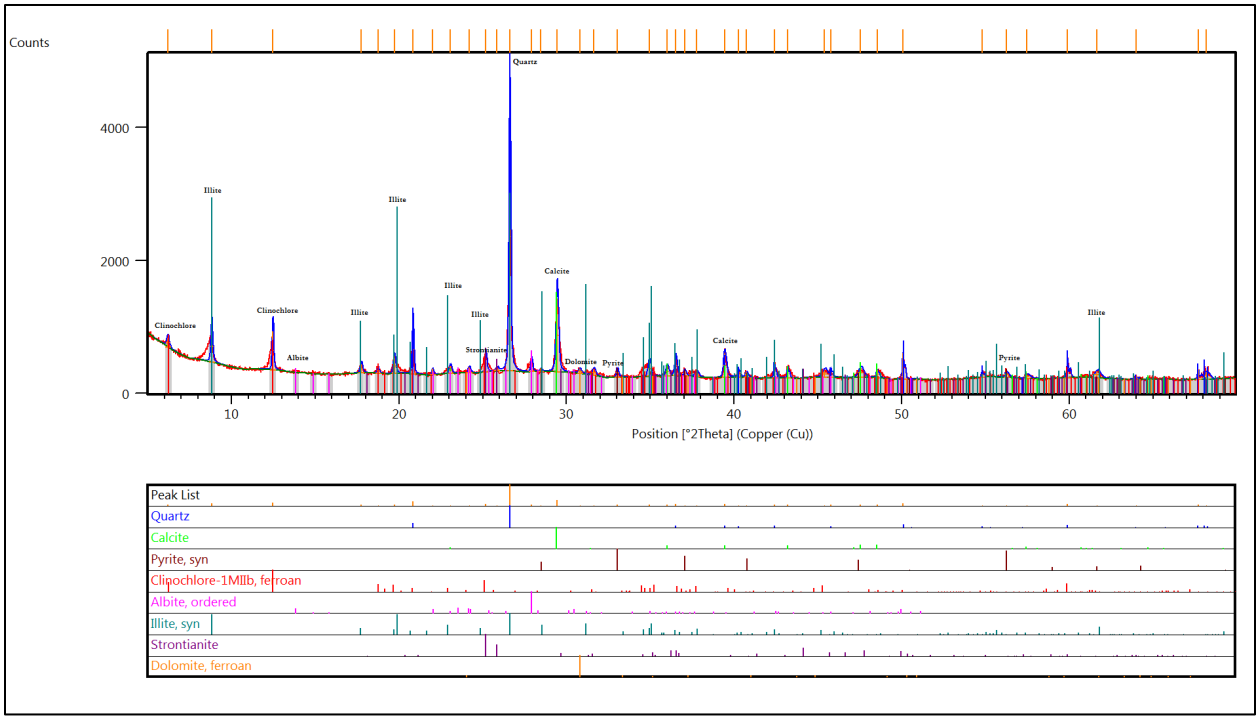

Figure 4: XRD scan for cuttings depth 8680 ft–8710 ft (one-quarter divergence slit)

3.1.2 Core Samples

The XRD scan for core depth 8549 ft shows a carbonate-rich mineralogy compared to the cuttings samples (Figure 5). Illite/muscovite are identified based on the 10-angstrom d-spacing peak at 9.01 degrees 2-theta. Calcite and dolomite are identified based on the 100 relative intensity lines at 29.43 and 30.98 degrees 2-theta, respectively, as well as the presence of most expected peaks over the entire 2-theta range of the scan. Calcite shows the highest peak intensity (counts) in core samples, as compared to cuttings samples where quartz is the highest intensity peak. Quartz is identified based on its 100 relative intensity line at 26.67 degrees 2-theta. Pyrite is evident based on the 1.63-angstrom d-spacing peak at 56.34 degrees 2-theta. The highest relative intensity (major) peak for albite is identified at 28.0 degrees 2-theta (d-spacing 3.19 angstroms), respectively. A 7-angstrom peak for amesite at 12.0 degrees 2-theta is also present.

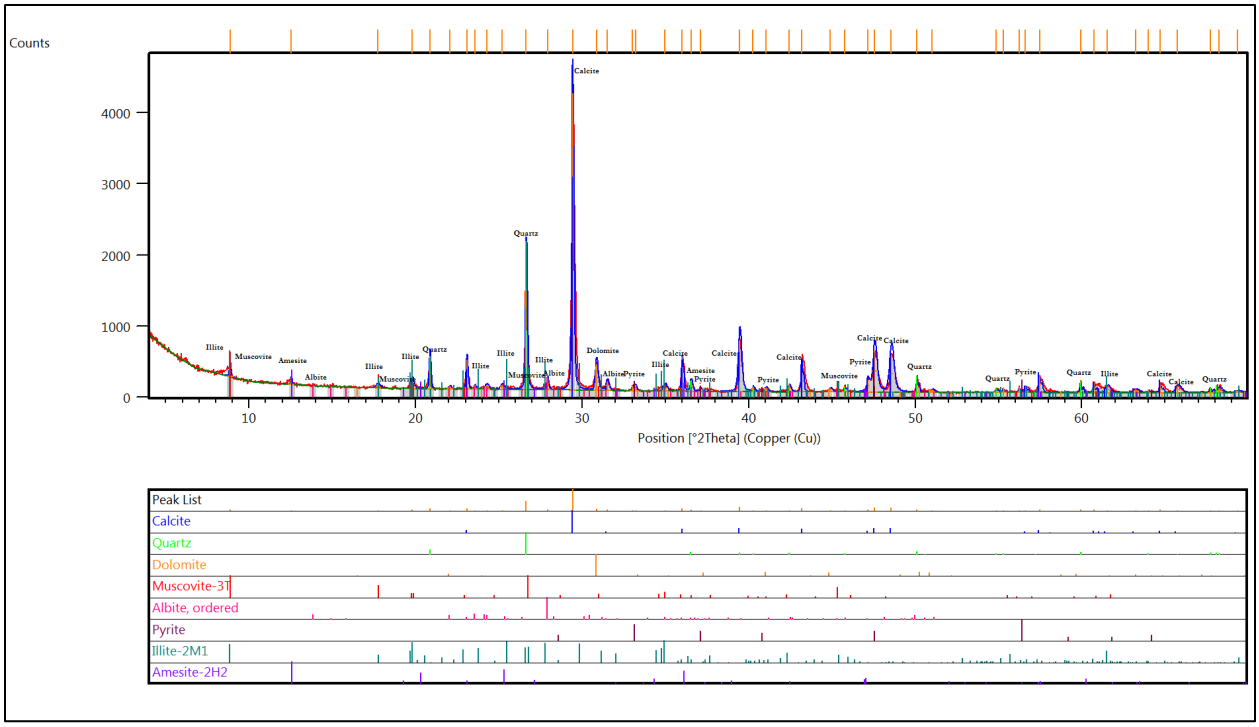

Figure(5): XRD scan for core (matrix and carbonate) depth 8549 ft

The XRD scan for core depth 8479 ft (carbonate) again shows a carbonate-rich mineralogy as compared to the cuttings samples (Figure 6). Muscovite is identified based on the 10-angstrom d-spacing peak at 9.01 degrees 2-theta. Calcite is again identified based on the 100 relative intensity line at 29.43 degrees 2-theta, and the occurrence of most expected peaks over the entire 2-theta range of the scan. Calcite shows strong overlap with magnesium calcite and chalcopyrite around 29.43 degrees 2-theta. Quartz is identified based on its 100 relative intensity line at 26.67 degrees 2-theta. Pyrite is evident based on the 1.63-angstrom d-spacing peak at 56.34 degrees 2-theta and its 2.71-angstrom d-spacing peak (85 relative intensity line) at 33.07 degrees 2-theta. The highest intensity (major) peak for ankerite ($Ca(Fe,Mg,Mn)(CO_3)_2$) is identified at 31.0 degrees 2-theta (d-spacing 2.91 angstroms).

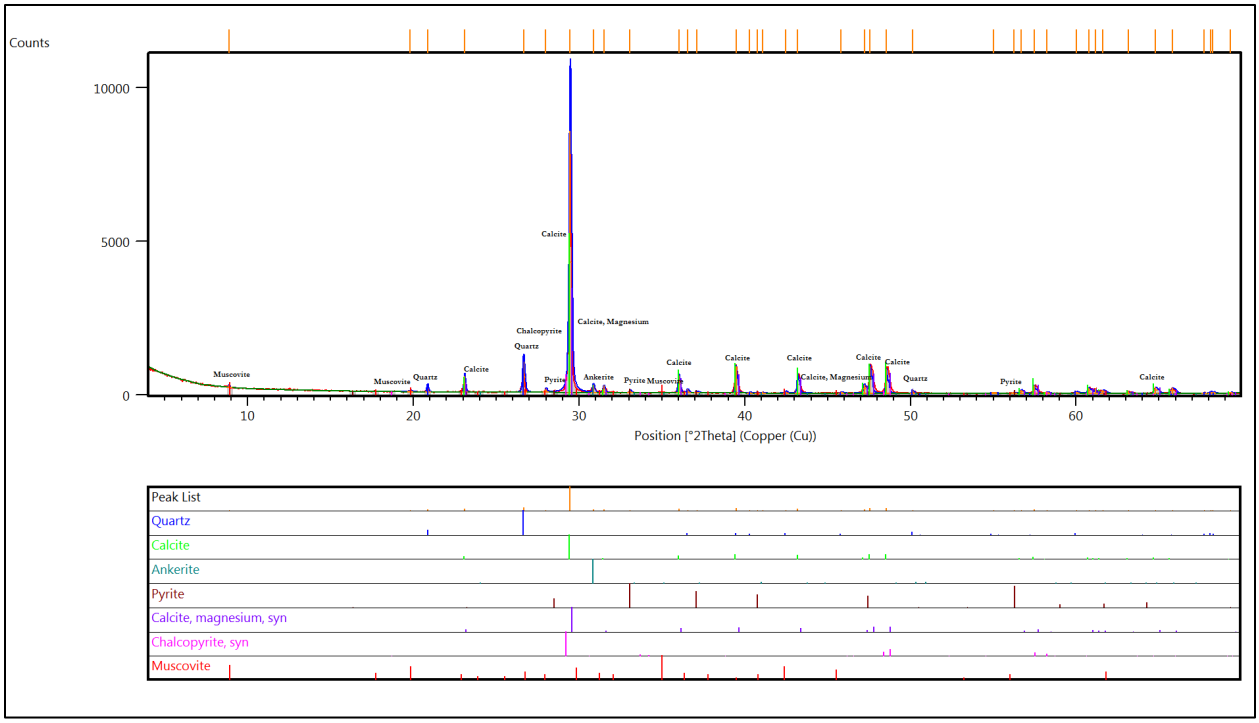

Figure 6: XRD scan for core (predominantly carbonate) depth 8479 ft

The XRD scan for core depth 8479 ft (matrix), shows a carbonate dominated mineralogy, similar to the previous core samples (Figure 7). Illite/muscovite and calcite and dolomite are once again identified at the respective 2-theta positions as in the first core scan. Quartz and pyrite again are present at the same 2-theta positions as in previous core scans. The highest intensity (major) peak for albite is identified at 28.0 degrees 2-theta, d-spacing 3.19 angstroms, respectively. A 12-angstrom peak for chamosite is also present. The scan for the clay-rich matix is given in Figure 7).

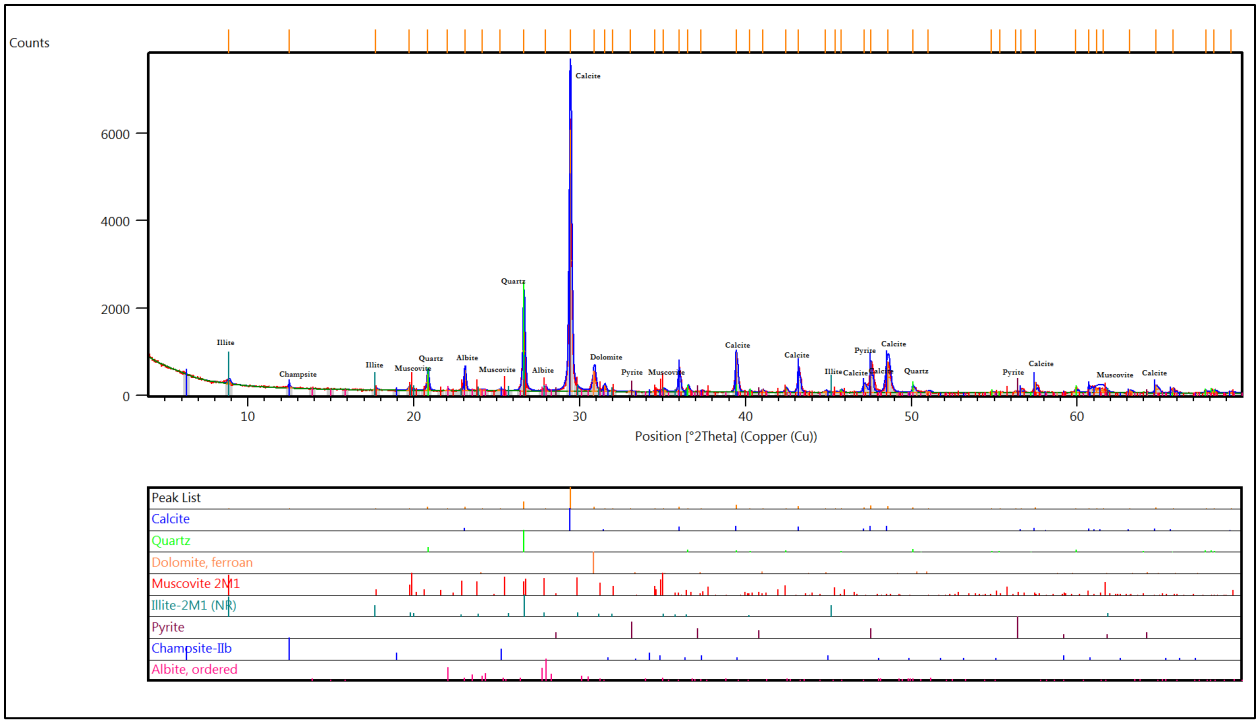

Figure 7: XRD scan for core (predominately fine-grained matrix) depth 8479 ft

3.2 Sequential Leach Experiments

For the water-rock experiments, three cuttings samples from the Utica Formation and two core samples from the Point Pleasant Formation were sequentially leached in water and dilute acid to determine the possible source of dissolved salts in flowback fluids. The results of these experiments show in general that the total solute release from the solid phase was greater in dilute acid than in water. The cuttings samples experiments in general had much higher solute concentrations than core using both water and acid leachates. Below is a summary of the results grouped by common element associations.

3.2.1 Calcium and magnesium

As seen in Figure 8a, the use of an acid as a leachate greatly affected the amount of calcium leached into solution. The source of calcium most likely is coming from calcium carbonate in both core and cuttings samples. The dissolution of calcite in acid can be written as follows:

$$CaCO_3 + 2H^+ \leftrightarrow Ca^{2+} + CO_2 + H_2O \qquad (1)$$

It became evident that too much acid was added during the set-up process for the fourth leach as there is a greater amount of calcium leached out compared to all other leaches. Perhaps the most important result from examining calcium concentrations is the affect that calcium carbonate had on the relative pH of acid samples. After the first and second leaches that were allowed to sit for 1 and 2 days, the pH of the acid leachates went from around a pH of 3 to a neutral pH. The buffering of the solution by calcite dissolution could explain this pH dependency. This is shown in Figure 8b.

As seen in Figure 8c, the use of an acid leachate affected the amount of magnesium leached out of solution but not to the same extent of calcium as seen above. The concentration of magnesium in solution depends on the initial solution pH, as magnesium in solution in the leach experiments is typically 2–3 times higher in the acid leach compared to the water leach experiments. However, this is much less than what was observed for calcium. In core samples, the magnesium concentration was higher in the acid leach compared to the water leach but the magnesium concentrations in subsequent leaches increased for all samples because the water-rock interaction time increased. In cuttings samples, the concentration of magnesium was again higher in acid samples as compared to water. The concentration stayed relatively the same after the first two leaches and then spiked after the third leach (2 weeks). These increases in concentrations over time

are most likely due to the dissolution of Mg-bearing calcite and/or dolomite. The dissolution of dolomite in acid can be written as follows:

$$CaMg(CO_3)_2 + 4H^+ \rightarrow Ca^{2+} + Mg^{2+} + 2CO_2 + 2H_2O \qquad (2)$$

Dissolution of other magnesium-bearing minerals identified in the XRD data, such as chlorite, could have contributed to the rapid increase after the third leach. Samples that used an acid leachate showed more magnesium after the fourth leach like with calcium above due to accidental addition of too much acid during the set-up process.

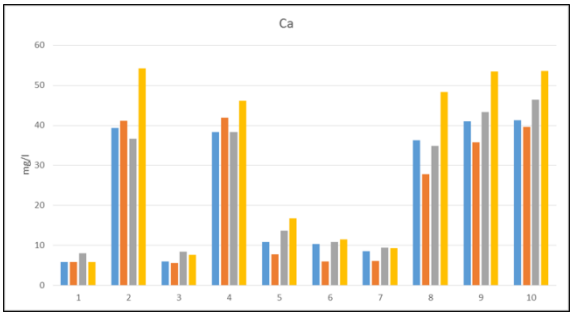

Figure 8a: Calcium concentrations M1-M10 Leaches 1-4

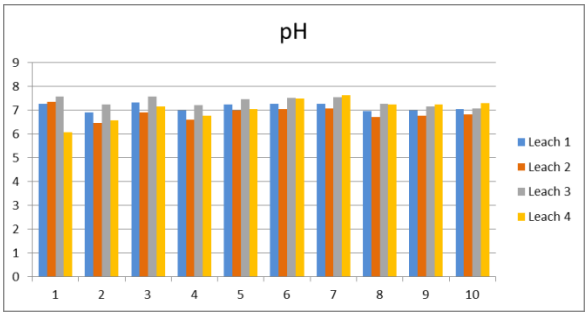

Figure 8b: Post-leach pH values

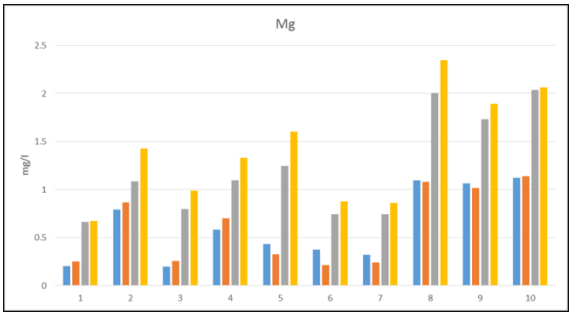

Figure 8c: Magnesium concentrations M1-M10 Leaches 1-4

3.2.2. Sodium and potassium

A large amount of sodium was leached out of both core and cuttings after the first leach (Figure 9a). In core samples, there was little to no sodium being dissolved after the second leach. Only a small amount of sodium dissolved in cuttings samples after the second and third leaches.

There was almost five times more sodium dissolved out of cuttings samples as compared to core. The decrease in concentrations in water from cuttings samples after the first leach compared to the increase in concentrations in acid cuttings samples could be a result of a mineralogical difference between the subsamples.

A large amount of potassium was leached out of both core and cuttings samples using both acid and water as a leachate (Figure 9b). In cuttings samples, there was a large amount of potassium that dissolved after the first leach. In core samples, an acid leachate leached out more potassium initially and then all sample concentrations slowly decreased for subsequent leaches, most likely because the reactive potassium phase present in the clays became depleted over time .In cuttings samples, potassium concentrations were lower after the first leach. The source of potassium in cuttings is most likely from drilling fluid used during hydraulic fracturing whereas the source of potassium in core is most likely from the illite/muscovite reactive clay phases present in the rock.

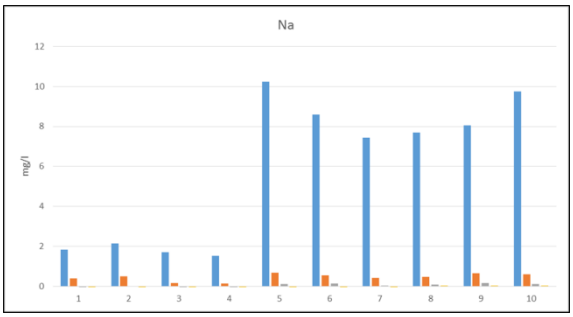

Figure 9a: Sodium concentrations M1-M10 Leaches 1-4

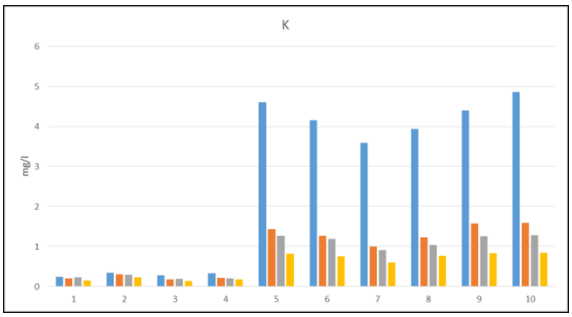

Figure 9b: Potassium concentrations M1-M10 Leaches 1-4

3.2.3 Strontium and barium

One of the most striking observations about the strontium concentrations is that they seem to be very similar to magnesium concentrations (Figure 10a). Reaction time seems to increase concentrations in core samples but deplete concentrations in cuttings samples. Perhaps cuttings

samples contained strontium that was not readily soluble due to a mineralogical difference. The leaching of strontium into solution is believed to follow calcium and magnesium because it is released during the dissolution of calcite and dolomite where it occurs as a minor constituent.

The barium concentrations were significantly higher in all cuttings samples as compared to core samples Figure(10b). However, barium dissolution from core samples is readily detected and shows trends that can be explained by increase in reaction time. Barium concentrations are not significantly higher in either the core or cuttings samples leached in acid and water.

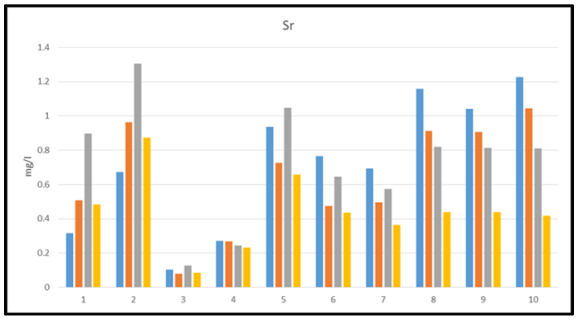

Figure(10a): Strontium concentrations M1-M10 Leaches 1-4

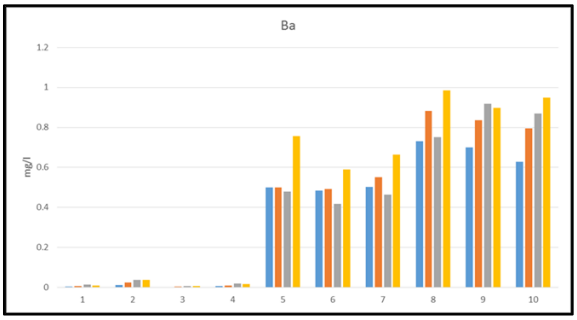

Figure(10b): Barium concentrations M1-M10 Leaches 1-4

3.2.4 Sulfate and chloride

A correlation is observed between the use of acid as a leachate and the lowering of the sulfate concentrations as compared to water samples (Figure 11a). Cuttings samples leached sulfate into solution by a factor of 1.5 times more than core. Over time, sulfate concentrations decreased in all samples until the third leach when concentrations seem to rise again. When comparing barium and sulfate relative to each other, it appears as if sulfate concentrations are lowered minimally by using an acid leachate but the use of acid actually increases the barium concentrations in the same samples. This trend occurs in both core and cuttings, but occurring a small amount more in cuttings. This suggests that there may be a reaction occurring between barium and sulfate.

The use of a hydrochloric acid leachate affected the amount of chloride present in both core and cuttings samples (Figure 11b). The amount of Chloride leached is not pH dependent. Chloride not only was leached out of the samples themselves but also more was present in all samples from the fourth leach which was due to accidentally adding too much acid as a result of either accidentally setting the automatic pipette wrong or using the wrong concentration of acid. The slow increase in chloride in acid leaches in both core and cuttings is a result of not entirely removing the supernatant solution for each leach in an attempt to preserve water-rock ratios. It is possible that the slow increase in chloride also is coming from the minerals in the samples that contain chloride in their bulk mineralogy.

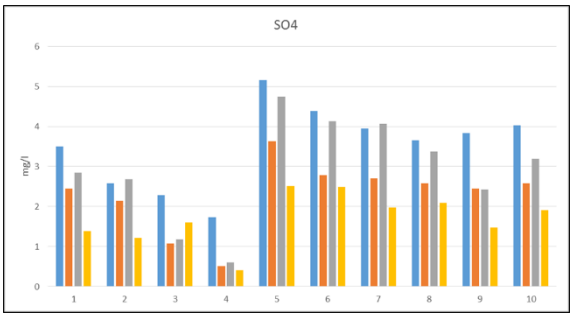

Figure 11a: Sulfate concentrations M1-M10 Leaches 1-4

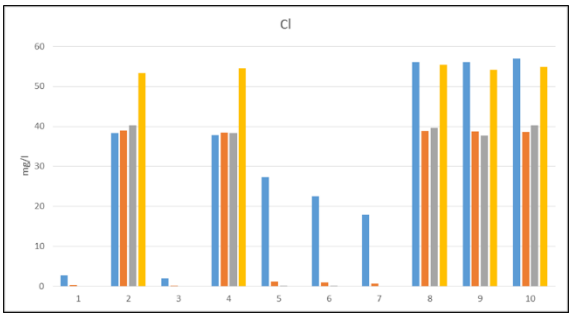

Figure 11b: Chloride concentrations M1-M10 Leaches 1-4

Figure 12a below shows the effect of using an acid as a leachate on core and cuttings samples when analyzing barium versus sulfate. Leaches 1, 2 and 4 are presented in Figures(1C), (2C) and (4C) in Appendix C. The same can be seen in figures (12b) and (12c) showing barium + strontium versus sulfate. This again shows the effect of using an acid as a leachate on core and cuttings samples. Leaches 1 and 4 are presented in Figures (5C) and (8C) in Appendix C.

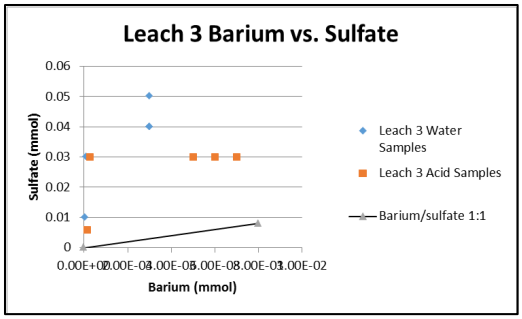

Figure 12a: Barium vs. Sulfate concentrations Leach 3

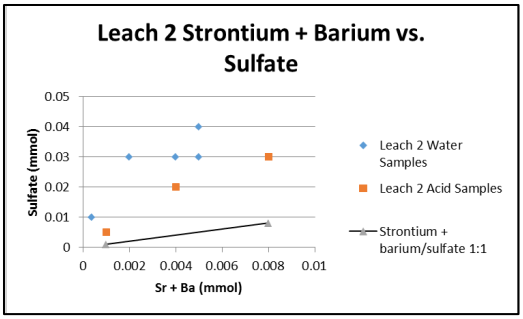

Figure 12b: Strontium + Barium vs. Sulfate concentrations Leach 2

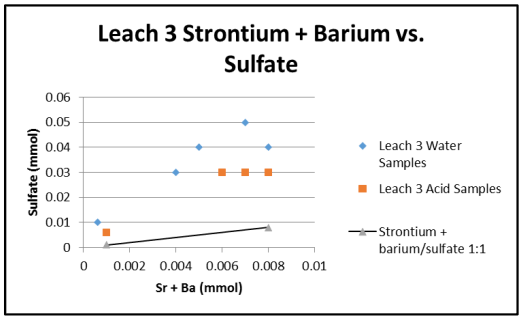

Figure 12c: Strontium + Barium vs. Sulfate concentrations Leach 3

3.3 Scanning Electron Microscopy (SEM) and Energy Dispersive X-Ray Spectrometry (EDXS)

Dried samples used in the sequential leach experiments were analyzed on the SEM to identify changes in the physical and chemical characteristics. Analysis was done to acquire mineral textural data and then specific grains were targeted using EDXS to acquire elemental data. The most surprising result was that there was still abundant barite in the cuttings samples, even after the fourth leach that had been allowed to react for three weeks. However, there was little to no barite detected in the in core samples. Figures 13 and 14 show significant amounts of barite present in sample M8, a cuttings sample leached in acid, as evident from the bright minerals in the BSED image. The elemental signatures were confirmed by using EDXS shown in Figure 15.

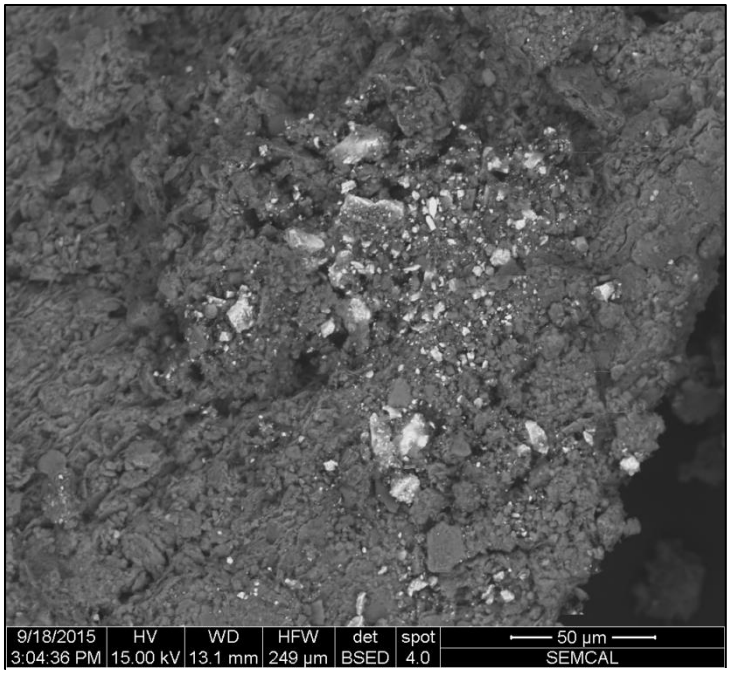

Figure 13: Cuttings sample leached in acid from depth 8470 ft-8500 ft in the Utica Formation showing a presence of barite represented by the bright grains in the BSED image.

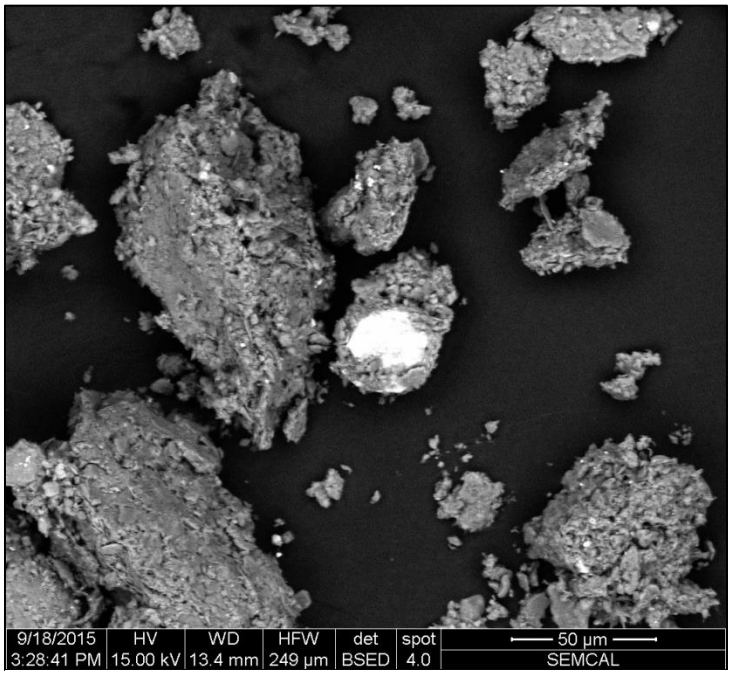

Figure 14: Cuttings sample leached in acid from depth 8470 ft-8500 ft in the Utica Formation showing a large, euhedral barite grain with smaller grains throughout the BSED image.

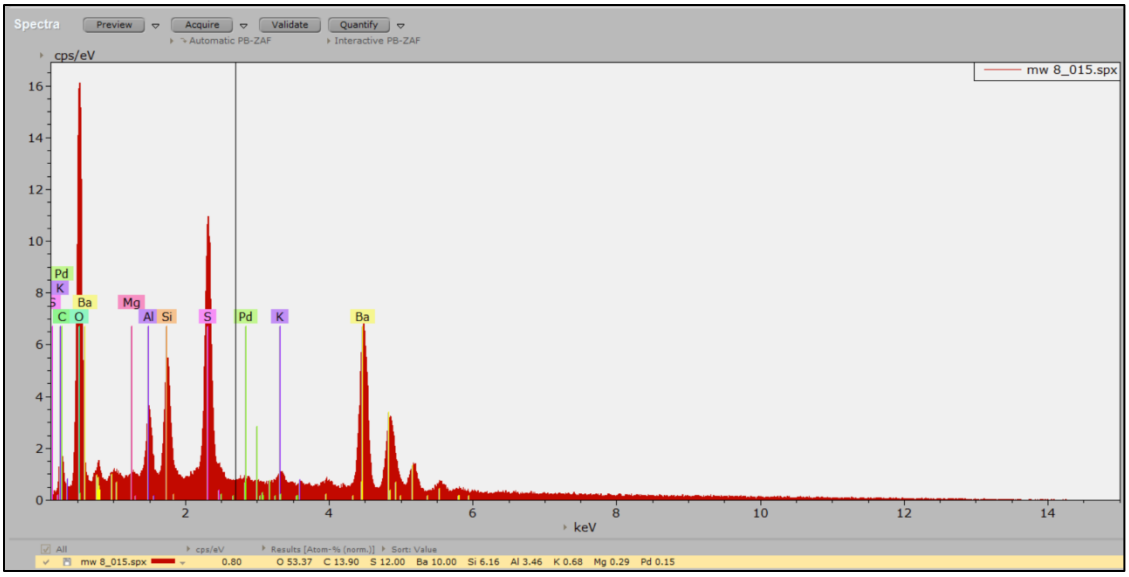

Figure 15: EDXS data showing chemistry of cuttings sample leached in acid from depth 8470 ft-8500 ft in the Utica Formation where spot analysis was taken on the large, euhedral grain presented in the BSED image.

The results proved the same when analyzing cuttings samples leached in only water as seen in Figures 16 and 17 below. Chemistry was confirmed using EDXS shown in Figure 18 below.

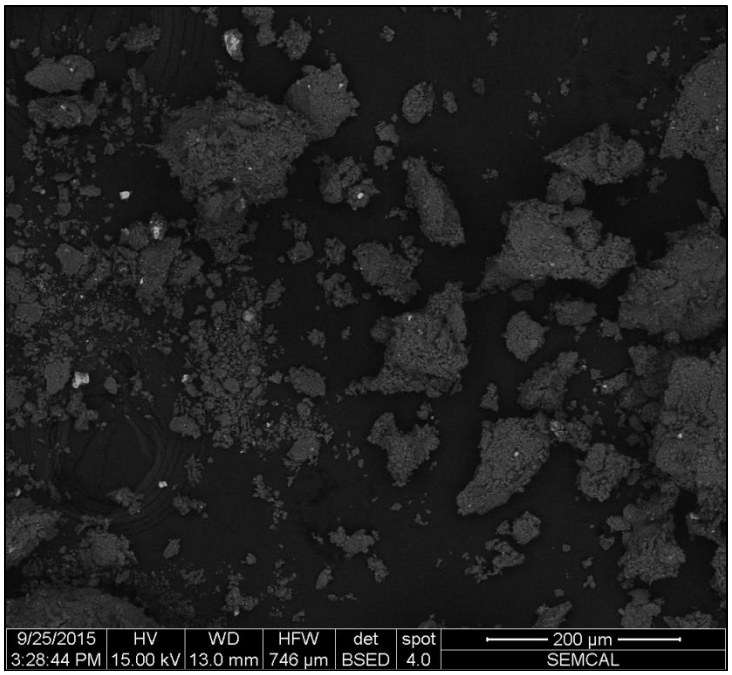

Figure 16: Cuttings sample leached in water from depth 8470 ft-8500 ft in the Utica Formation showing barite grains throughout the BSED image.

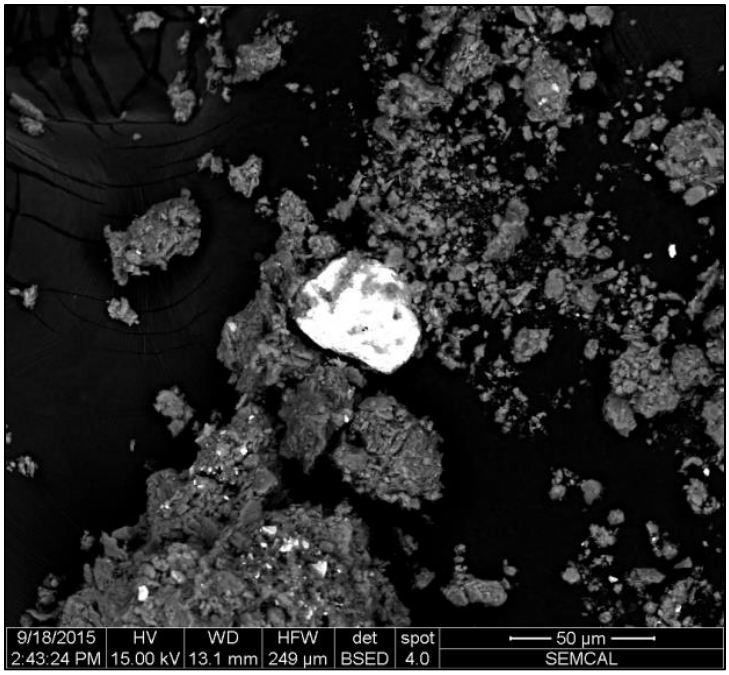

Figure 17: Cuttings sample leached in water from depth 8500 ft-8530 ft in the Utica Formation showing a large, euhedral barite grain with smaller grains throughout the BSED image.

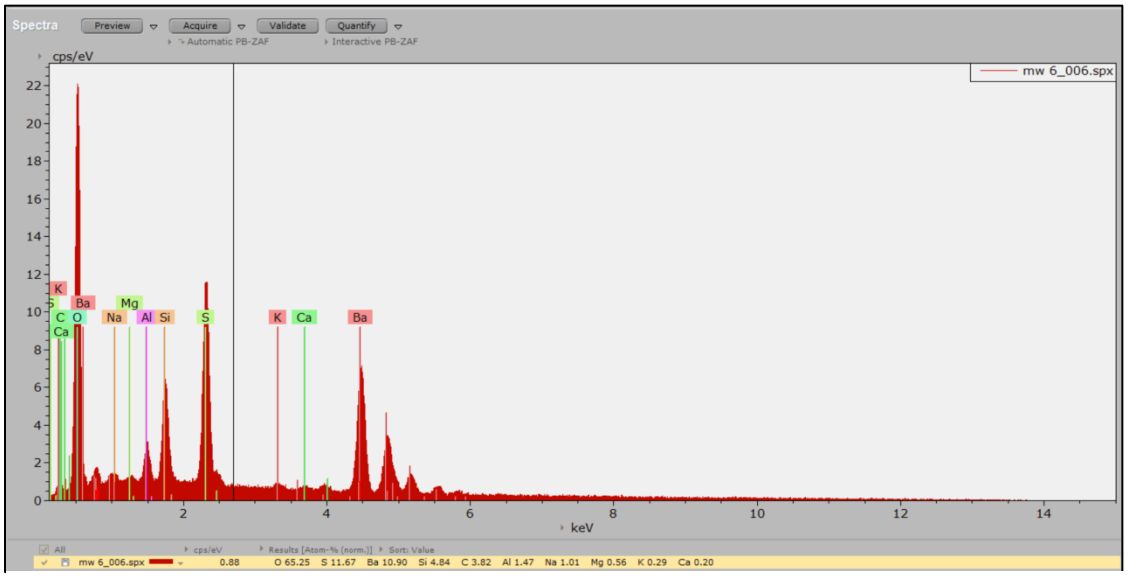

Figure 18: EDXS data showing chemistry of cuttings sample leached in water from depth 8500 ft-8530 ft in the Utica Formation where spot analysis was taken on the large, euhedral grain presented in the BSED image.

SEM analysis was also performed on core samples. Core samples, like the one presented in Figure 19, exhibited dissolution textures which can be tied to the mineralogy of the sample. The mineralogy was confirmed using EDXS spot analysis (Figure 20).

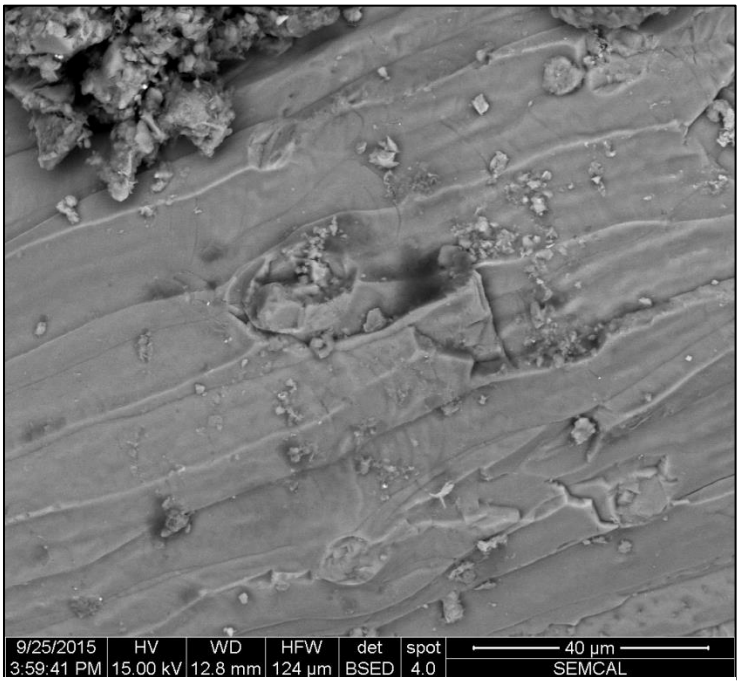

Figure 19: Core sample leached in acid from depth 8479 ft in the Point Pleasant Formation showing dissolution textures throughout the BSED image.

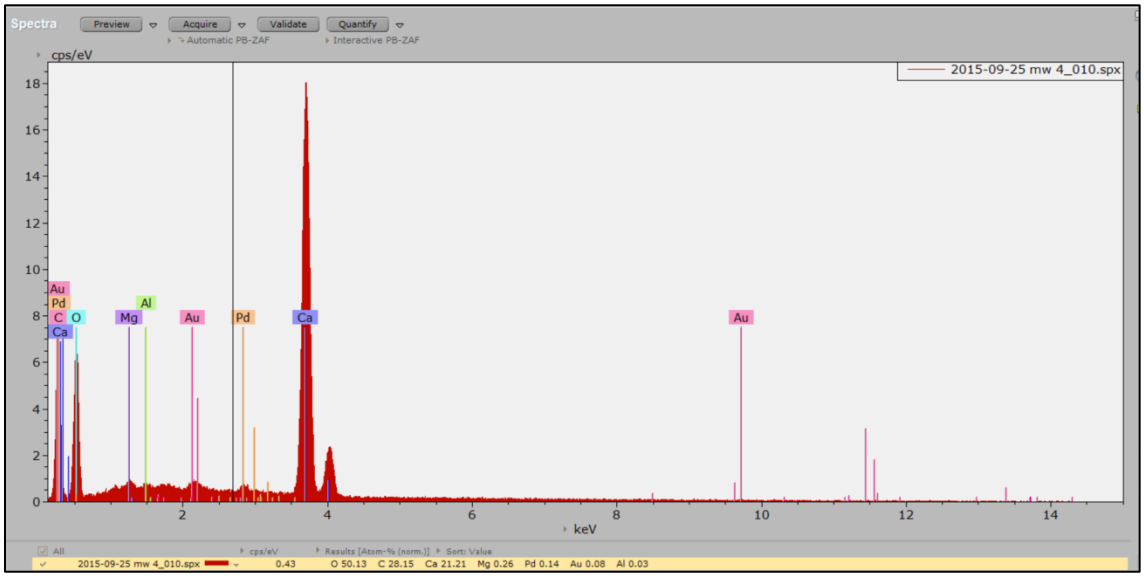

Figure 20: EDXS data showing calcium carbonate chemistry of core sample leached in acid from depth 8479 ft in the Point Pleasant Formation where spot analysis was taken on the dissolution surface presented in the BSED image.

Pyrite framboids were evident when scanning over the samples and were easy to identify. This result confirms the XRD data for core samples that indicated the presence of significant amounts of pyrite. Its image and corresponding EDXS spot analysis are presented in Figures 21 and 22.

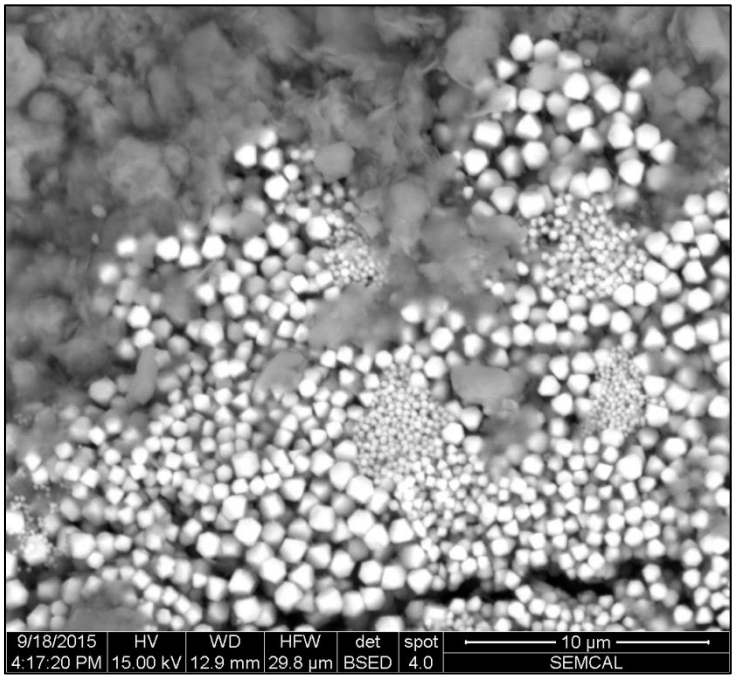

Figure 21: Acid-leached core sample from depth 8549 ft in the Point Pleasant Formation showing pyrite framboids surrounded by illitic clay throughout the BSED image.

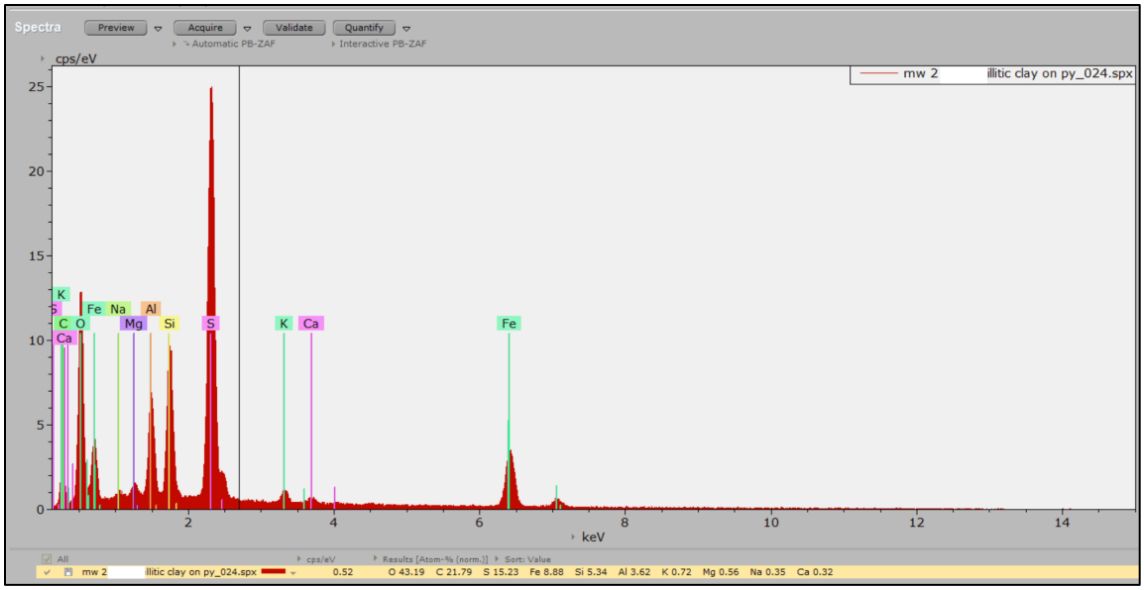

Figure 22: EDXS data confirming pyrite presence in core sample leached in acid from depth 8549 ft in the Point Pleasant Formation where spot analysis was taken on the bright framboids presented in the BSED image.

3.4 PHREEQC Geochemical Modeling

The use of PHREEQC geochemical modeling software allowed for the analysis of saturation indices for relevant minerals in this experiment. Initial inputs are represented in Tables 1E-4E in Appendix E. All phase saturations for samples and leaches are presented in Tables 5E-44E in Appendix E. Mineral saturations were analyzed for phases aragonite, calcite, dolomite, barite, celestite, gypsum and strontianite. The use of a dilute acid leachate effectively brought the phases closer to saturation than by using only water. The most important observation made from this modeling procedure was that barite proved to be near perfect saturation in all cuttings samples after the fourth leach.

4. Discussion

As stated previously, cuttings samples had been chosen as a means of correlation to core samples from the pay zone. It was discovered later on that cuttings samples and core samples were indeed from two different formations. This provided a new opportunity to compare and contrast organic-bearing shales that differ in bulk mineralogy such as in this experiment; the clay-rich Utica Formation vs. the carbonate-rich Point Pleasant Formation.

Results from Utica Formation cuttings samples analyzed showed a clay-rich consistency evident initially in XRD results. Clay-rich phyllosilicate minerals such as illite, muscovite and chlorite dominate bulk mineralogy. Cuttings samples leached large amounts of calcium, magnesium, sodium, potassium, barium, strontium and sulfate and chlorine. Acid used as a leachate proved to leach these readily soluble minerals into solution more than using only water, although a fair amount still leached into solution with water and almost all samples leached more than core samples with the exception of magnesium, calcium, chlorine and strontium. Acid affected the carbonates in a way that caused fast dissolution of calcite and dolomite. This rapidly effected pH, as the acid leachate with an initial pH of 3 started neutralizing to a pH of around a 7. This change occurred within approximately one day. Fast neutralization of pH from carbonate dissolution consequently effected pH dependency of proceeding minerals leached into solution to having almost no dependence. However, calcium and magnesium both show strong pH dependence as is evident in the results. Cuttings samples showed a large presence of barite in SEM images that was not evident in core samples although that does not rule out its presence core samples.

Results from Point Pleasant Formation core samples analyzed showed a carbonate rich consistency as indicated in the XRD results where the calcite and dolomite dominate bulk mineralogy with some minor clays and pyrite. Core samples leached reasonable amounts of calcium,

magnesium, sodium, potassium, barium, strontium, sulfate and chlorine. Acid equally affected carbonate dissolution in core samples as in cuttings samples. SEM analysis showed evidence of dissolution pits in areas proven to be calcite in core acid samples. Core and cuttings samples proved to be leaching salts such as calcium chloride, sodium chloride and potassium chloride. A recent study by Blauch et. al (2009) on the Marcellus shale states that post-fracking flowback waters are characterized by sodium chloride and calcium chloride waters from brine deposits formed from evaporated seawater within the formation due to fluid mobilization into it. It is also stated that dolomitization occurs from water-rock interactions from diagenetic processes. One can argue that calcite and dolomite from samples in this thesis experiment originate from the Utica and Point Pleasant Formations themselves as their dissolution rates seem to be relatively the same in core and cuttings samples. A hypothesis for the source of additional magnesium in cuttings samples is that it may have originated from chlorite that is omnipresent in cuttings samples as seen in XRD results. Calcium chloride and sodium chloride also could be originating from natural formation salts. Interestingly, Blauch et al. (2009) also found that barite, calcite, and dolomite were all saturated with respect to themselves. The use of PHREEQC in this thesis experiment showed similar results however, barite did not become saturated until it was leached out of cuttings samples. Calcite, dolomite and celestite remain under saturated with respect to themselves. Because of the striking difference in barite concentrations between core samples and cuttings samples, it is hypothesized that the majority of barite was introduced during the fracturing process. This hypothesis holds the same for the presence of potassium only it cannot be ruled out that potassium in core samples is from the minor illite/muscovite clay phases present in the formation. The source of strontium can be hypothesized to be coming from the formation itself because it is known to follow calcium and magnesium. It can be concluded that an acid leachate was the most influential variable on the release

of carbonates and sodium, calcium and potassium chlorides and time were the most influential variables for the release or depletion of all other minerals such as barium, strontium and sulfate.

5. Suggestions for Future Research

Presently, sequential leach experiments are being performed on a new set of samples. All samples being used are from the same core and cutting depths as the core and cutting samples used for this thesis experiment. Unfortunately, the set-up and analysis of these experiments could not be finished before this thesis was published. Description of the work already performed on the samples and the future steps to be included in the experiments are described below. Additional suggestions for future work will also be discussed.

Samples and their corresponding depths are represented in Table 3:

Table 3: Samples used and their corresponding depths

Depths of Samples	
Sample Numbers	Sample Depths (ft)
M1 and M2	8549
M3 and M4	8479
M5 and M8	8470 ft-8500 ft
M6 and M9	8500 ft-8530 ft
M7 and M10	8530 ft-8560 ft

The sample weights for this experiment are different, however, from the weights used in the sequential leaches for this thesis experiment. Weights of samples are represented in Table 4:

Table 4: Pre- hard leach sample weights

Weights of Samples Pre-Leach	
Sample Number	Weight (g)
M1	0.533 g
M2	0.528 g
M3	0.584 g
M4	0.593 g
M5	0.508 g
M6	0.518 g
M7	0.526 g
M8	0.508 g
M9	0.509 g
M10	0.576 g

Preparation of samples followed the same set-up procedures as the samples used in this thesis experiment. The experiment in progress follows the procedures of a similar experiment performed by Stewart et al. (2015) in which fluids injected during hydraulic fracturing are replicated in a lab.

For this experiment, the samples undergoing water leaching had been set up months prior and were allowed to sit for 5 months, 17 days. Samples M2, M4, M8, M9 and M10 were not used for this experiment as they contain acid with the same water-acid ratio used in this thesis experiment and would not follow the procedures described by the Stewart et al. (2015). Acid samples were set aside and left to dry after fluid to be analyzed was removed and will be prepped for future SEM analysis. Fluid from water samples M1, M3, M5, M6 and M7 was removed to be analyzed in the future and a new leachate was prepared following the second step in the journal being replicated. The purpose of the water leach in step 1 was to extract soluble salts and evaporated pore water. Step 2 was then set up by preparing ammonium acetate with a pH of 8. pH of ammonium acetate was tested and corrected to acquire a value close to a pH of 8. Initial pH value obtained was 7.13 and a dropper of ammonium hydroxide was added and pH was tested again with a new acquired value of 7.8. Approximately 50 mL of the ammonium acetate solution was added to the samples. Samples were shaken approximately 50 times to ensure rock and water were thoroughly mixed. This second step leach was then allowed to sit for 3 days. Fluid was then removed to be analyzed in the future. All fluids were removed following the same process used for this thesis experiment. The purpose of the ammonium acetate leach in step 2 was to extract surface exchangeable and low-charge interlayers.

Future leachates to be added and removed from the samples for future analysis include 8% acetic acid with a purpose to extract carbonate minerals, 0.1M HCl with a purpose to extract high-

charge interlayers and partial silicate/oxides and a total dissolution using HF, HNO_3 and $HClO_4$ with a purpose to extract silicates and remaining refractory minerals.

References Cited

Blauch, M. E., Meyers, R. R., Moore, T. R., Lipinski, B. A., & Houston, N. A. (2009). Marcellus Shale Post-Frac Flowback Waters – Where is All the Salt Coming From and What are the Implications? *Society of Petroleum Engineers.*

Stewart, B. W., Chapman, E. C., Capo, R. C., Johnson, J. D., Graney, J. R., Kirby, C. S., et al. (2015). Origin of brines, salts and carbonate from shales of the Marcellus Formation: Evidence from geochemical and Sr isotope study of sequentially extracted fluids. *Applied Geochemistry, 60*, 78-88.

Vazquez, O., Mehta, R., Mackay, E., Linares-Samaniego, S., Jordan, M., & Fidoe, J. (2014). Post-frac Flowback Water Chemistry Matching in a Shale Development. *Society of Petroleum Engineers.*

Welch, K. A., Lyons, W. B., Graham, E., Neumann, K., Thomas, J. M., & Mikesell, D. (1996). Determination of major element chemistry interrestrial waters from Antarctica by ion chromatography. *Journal of Chromatography A*, 739, 257–263.

Wilke, F. D. H., Vieth-Hillebrand, A., Naumann, R., Erzinger, J., & Horsfield, B. (2015). Induced mobility of inorganic and organic solutes from black shales using water extraction: Implications for shale gas exploitation. *Applied Geochemistry, 63*, 158-168.

Appendix A

Sample Description Tables

Table 1A: Samples and their corresponding depths, formations, leachates and type

Sample Number	Depth (ft)	Formation	Leachate Used	Type
M1	8549 ft	Point Pleasant	Water	Core
M2	8549 ft	Point Pleasant	Acid	Core
M3	8479 ft	Point Pleasant	Water	Core
M4	8479 ft	Point Pleasant	Acid	Core
M5	8470 ft-8500 ft	Utica	Water	Cuttings
M6	8500 ft-8530 ft	Utica	Water	Cuttings
M7	8530 ft-8560 ft	Utica	Water	Cuttings
M8	8470 ft-8500 ft	Utica	Acid	Cuttings
M9	8500 ft-8530 ft	Utica	Acid	Cuttings
M10	8530 ft-8560 ft	Utica	Acid	Cuttings

Table 2A: XRD samples and their corresponding depths, formations and type

Samples used for XRD Analysis		
Depth (ft)	**Formation**	**Type**
8549 ft	Point Pleasant	Core
8479 ft	Point Pleasant	Core
8410 ft-8440 ft	Utica	Cuttings
8500 ft-8530 ft	Utica	Cuttings
8680 ft-8710 ft	Utica	Cuttings

Table 3A: Pre-leach sample weights

Weights of Samples Pre-Leach	
Sample Number	Weight (g)
M1	0.541 g
M2	0.521 g
M3	0.551 g
M4	0.412 g
M5	0.577 g
M6	0.554 g
M7	0.477 g
M8	0.421 g
M9	0.468 g
M10	0.567 g

Table 4A: Pre- hard leach sample weights

Weights of Samples Pre-Leach	
Sample Number	Weight (g)
M1	0.533 g
M2	0.528 g
M3	0.584 g
M4	0.593 g
M5	0.508 g
M6	0.518 g
M7	0.526 g
M8	0.508 g
M9	0.509 g
M10	0.576 g

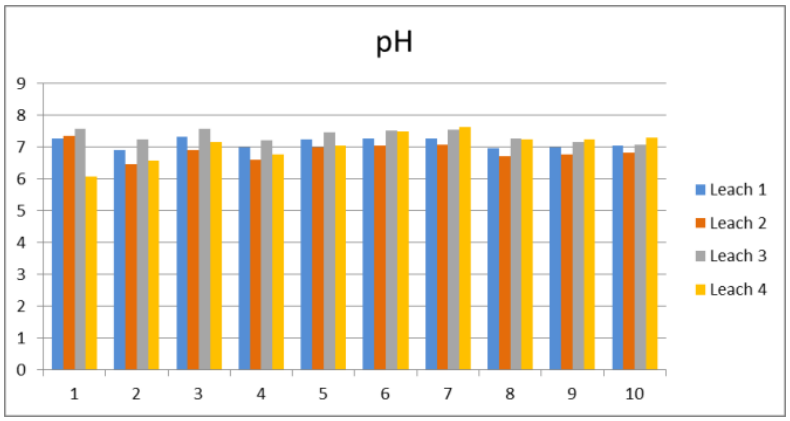

Figure 1A: Post-leach pH values

Appendix B

XRD Results

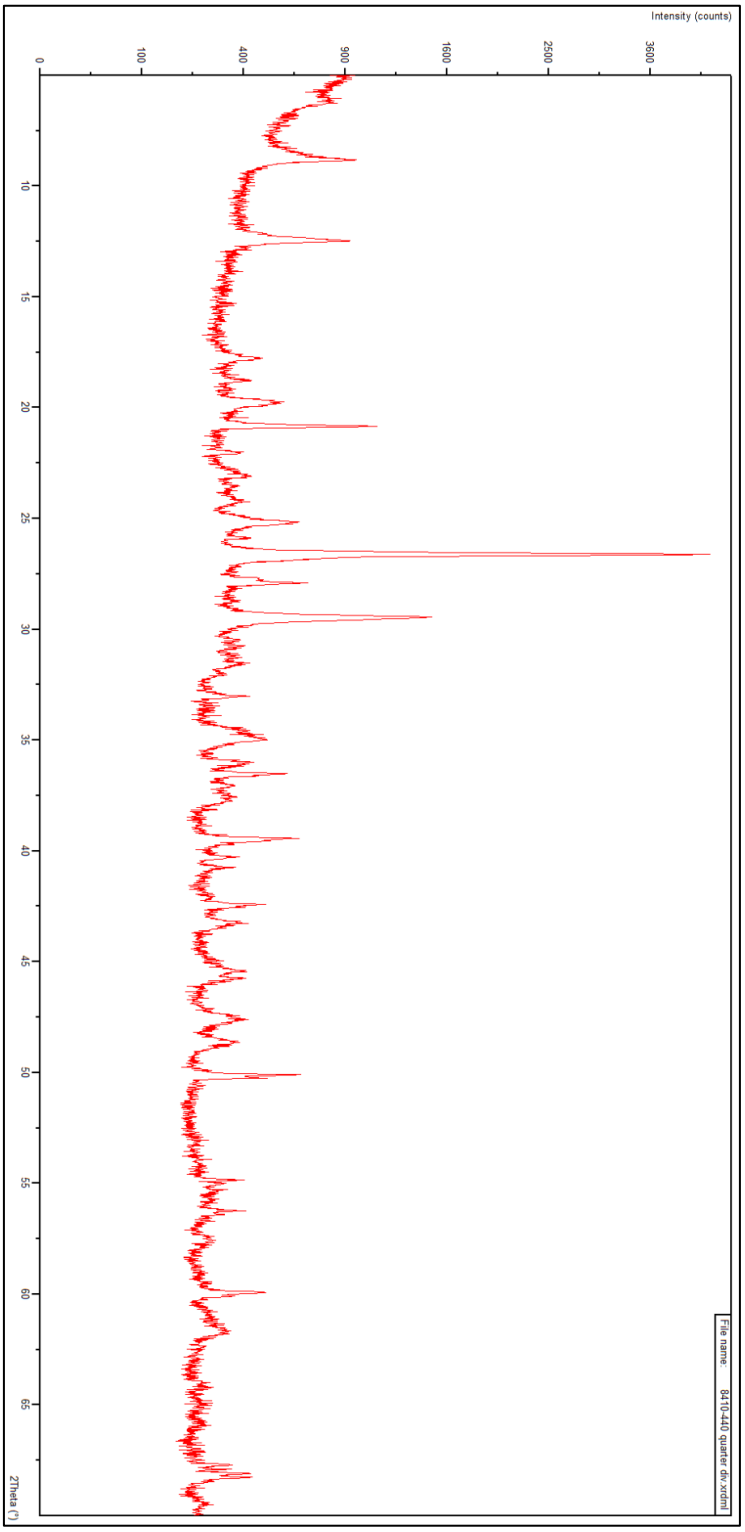

Figure 1B: Cuttings 8410 ft-8440 ft quarter divergence raw data

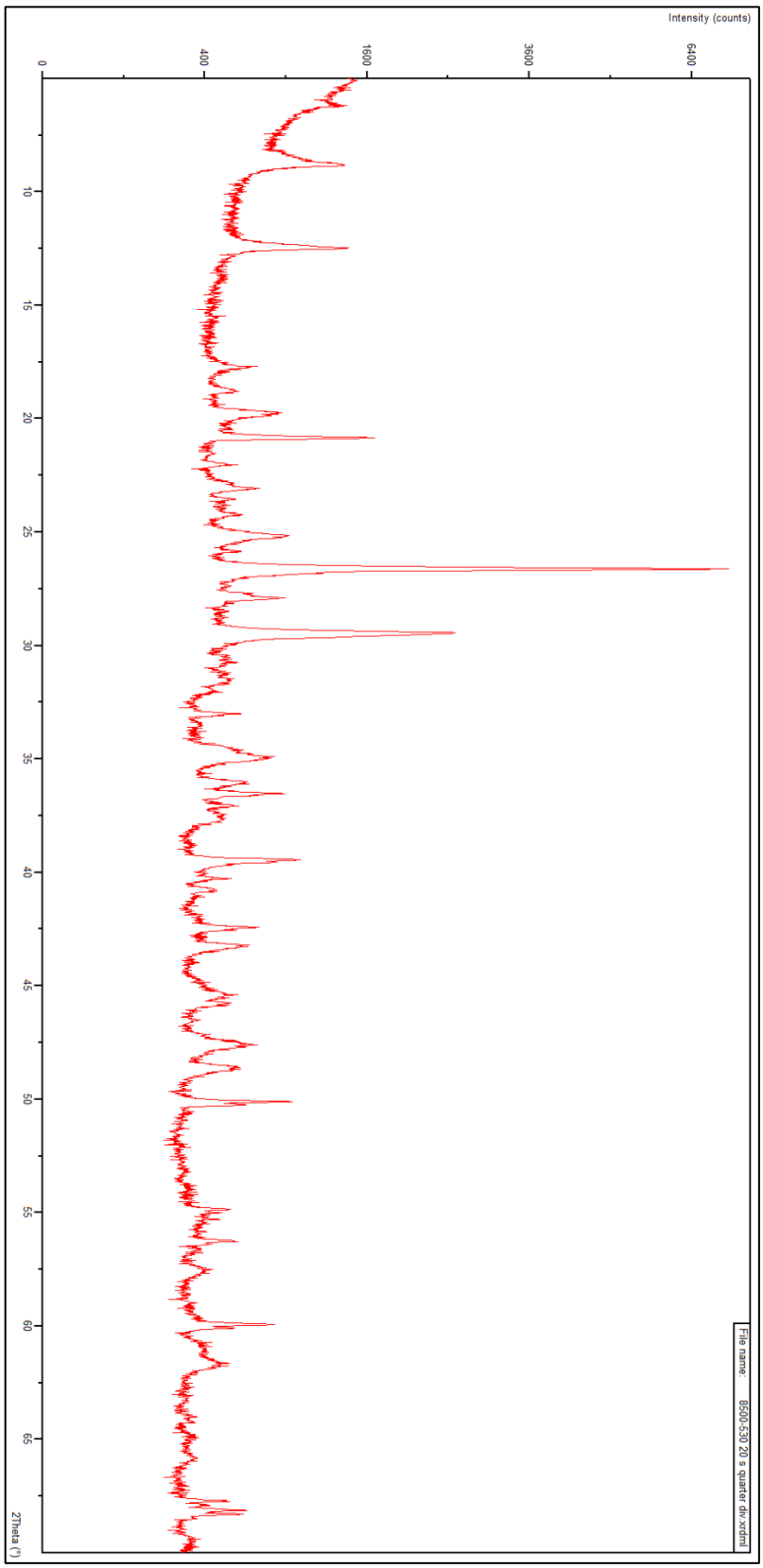

Figure 2B: Cuttings 8500 ft-8530 ft 20s quarter divergence raw data

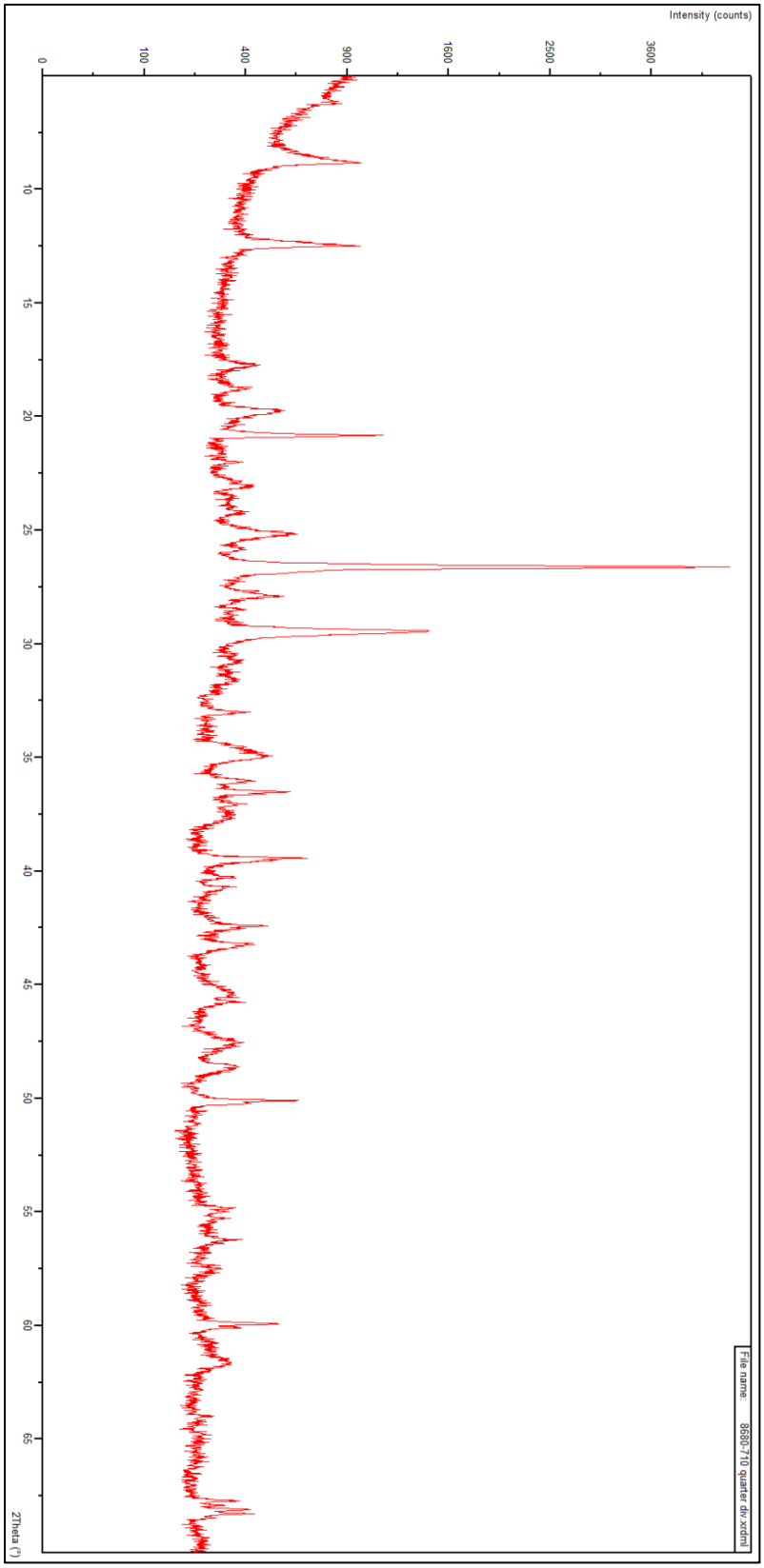

Figure 3B: Cuttings 8680 ft-8710 ft quarter divergence raw data

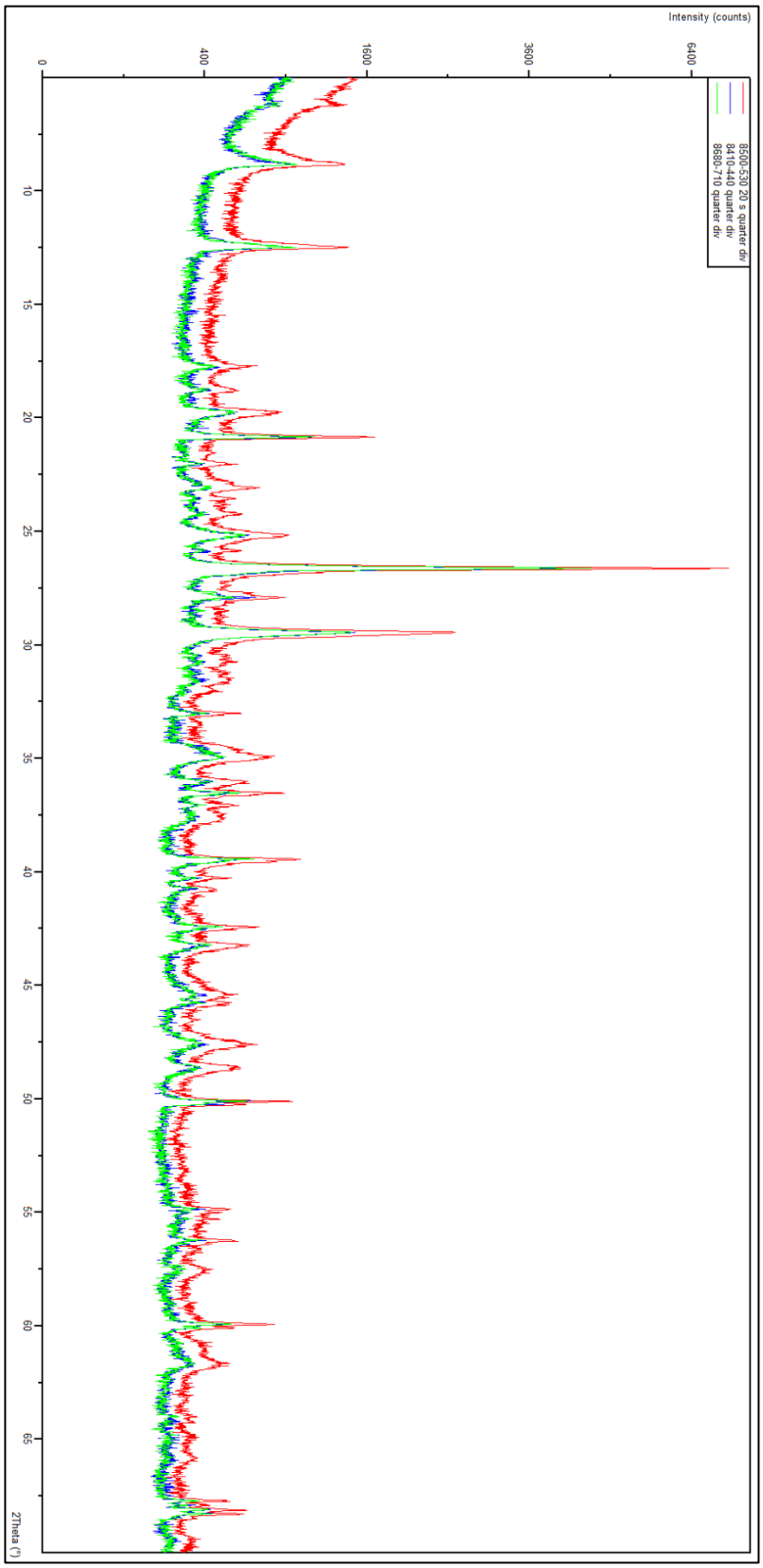

Figure 4B: Combined cuttings quarter divergence raw data

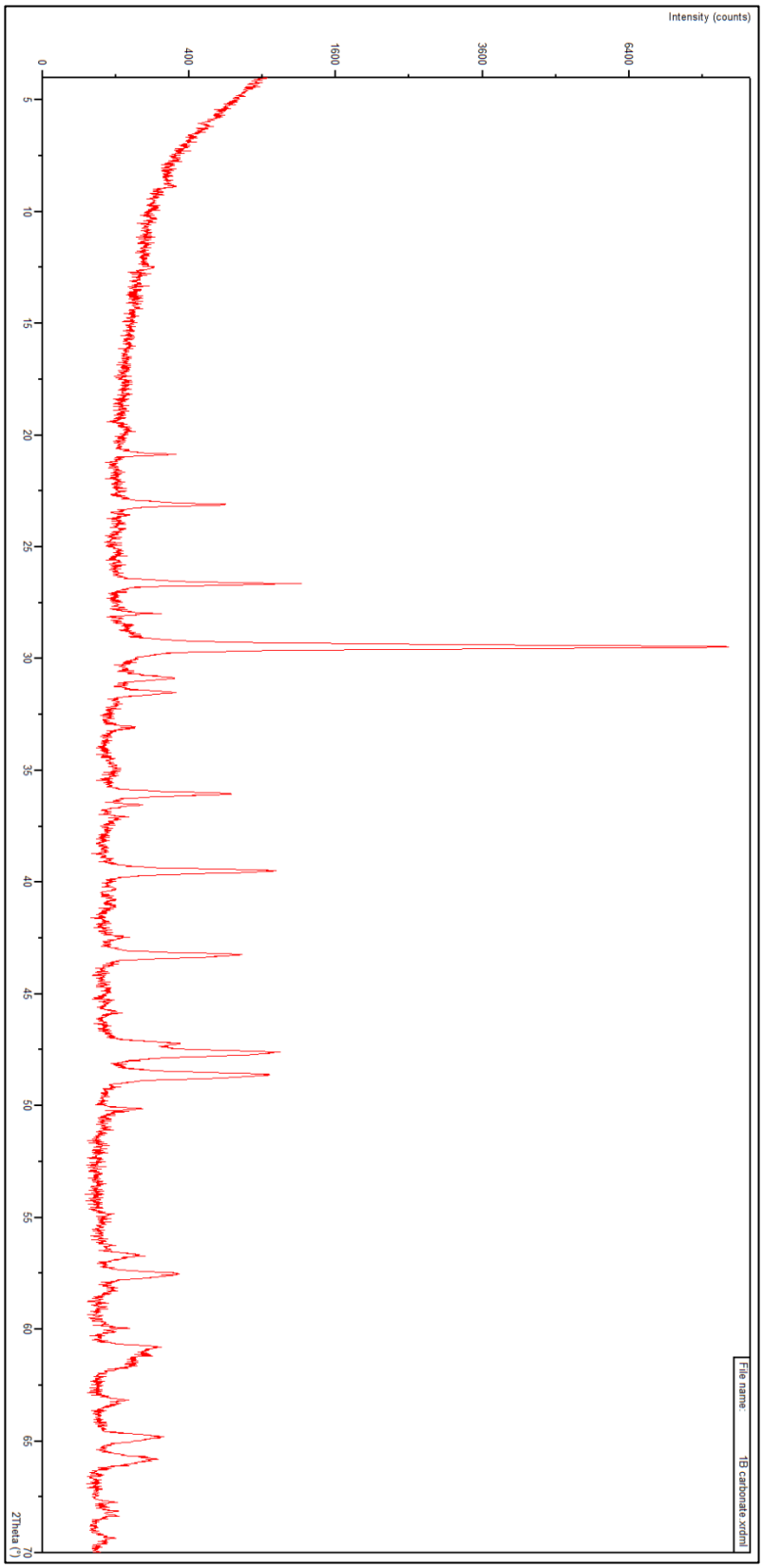

Figure 5B: Core (carbonate) 8479 ft raw data

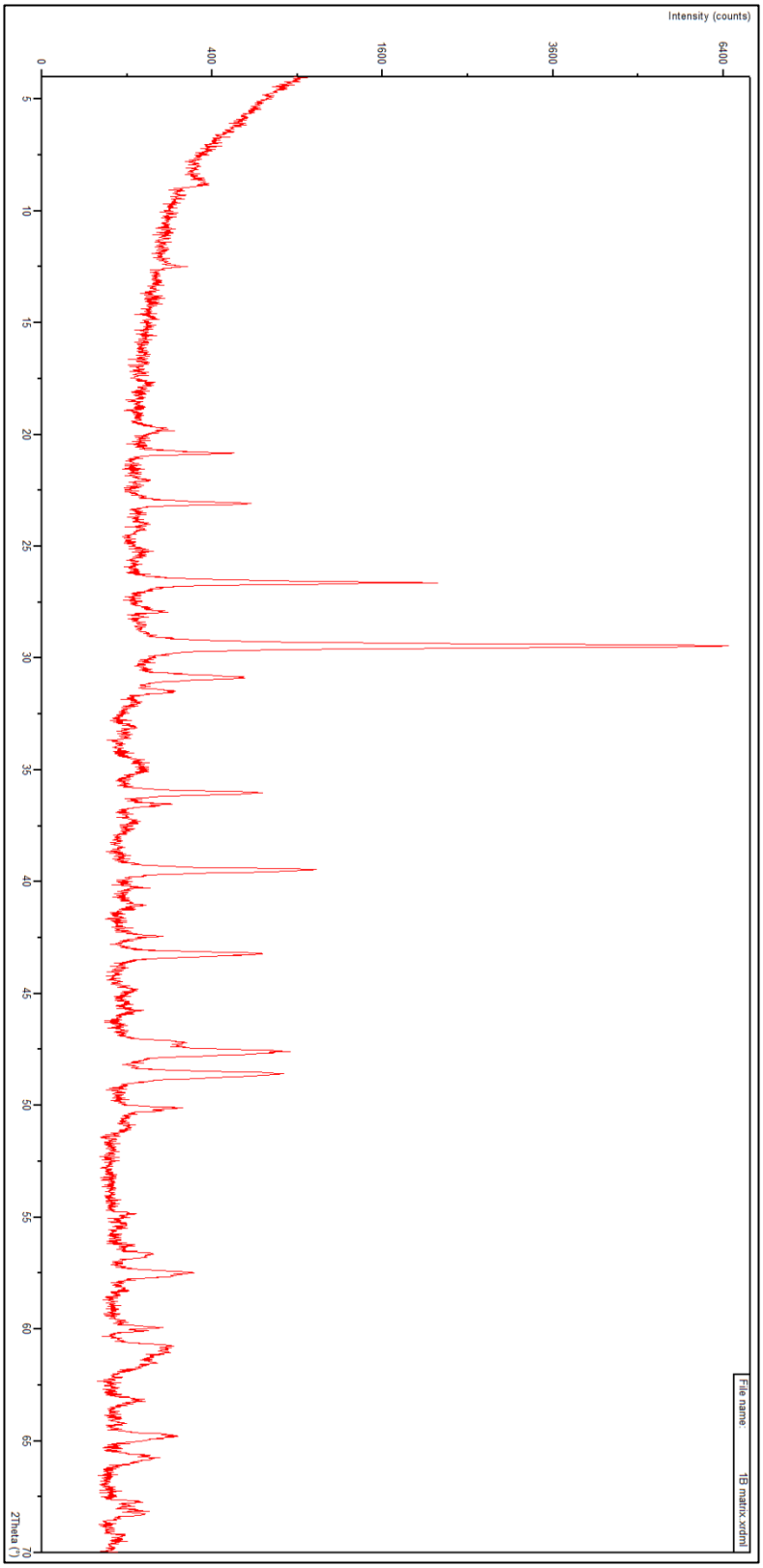

Figure 6B: Core (matrix) 8479 ft raw data

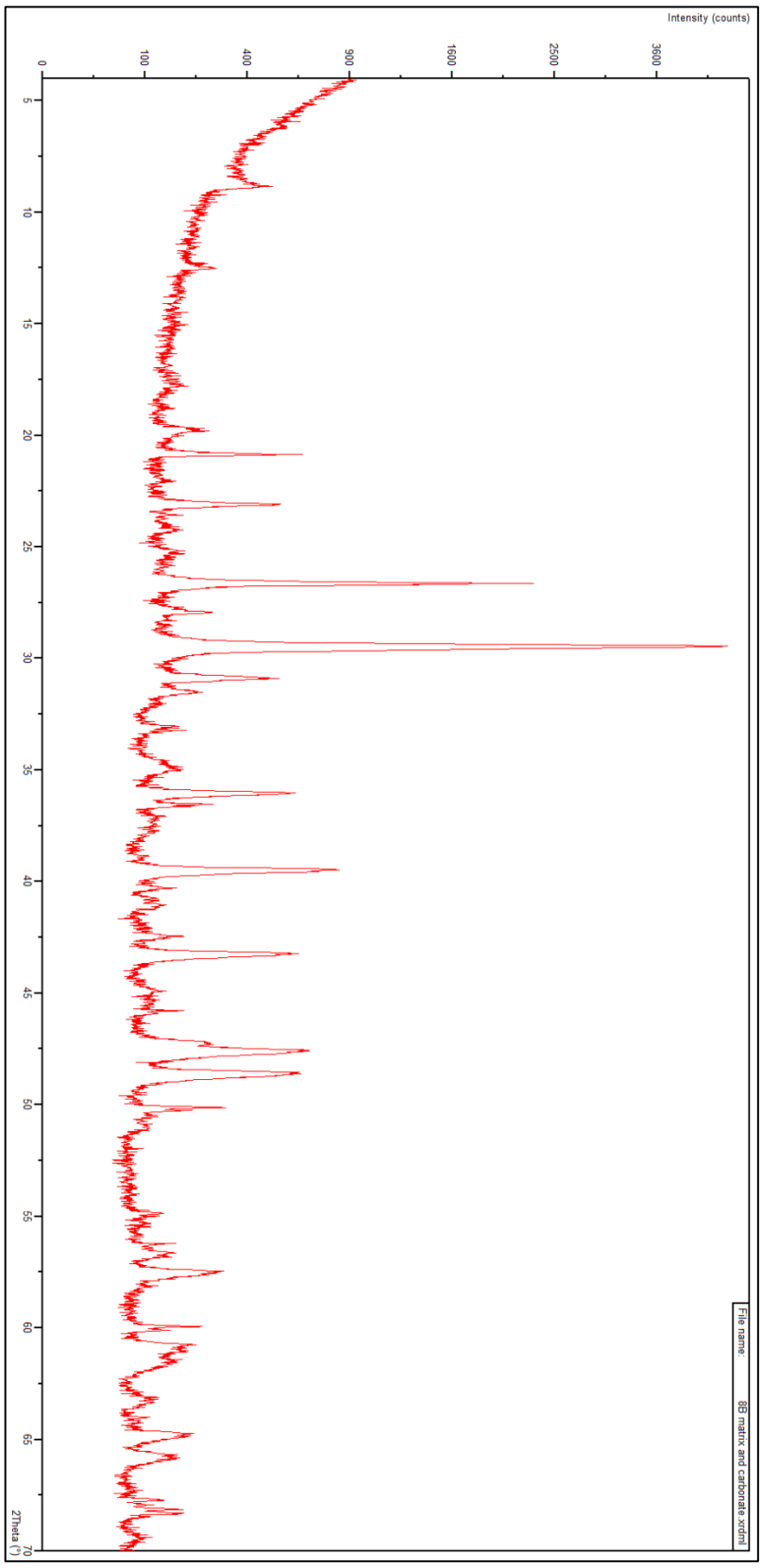

Figure 7B: Core (matrix and carbonate) 8549 ft raw data

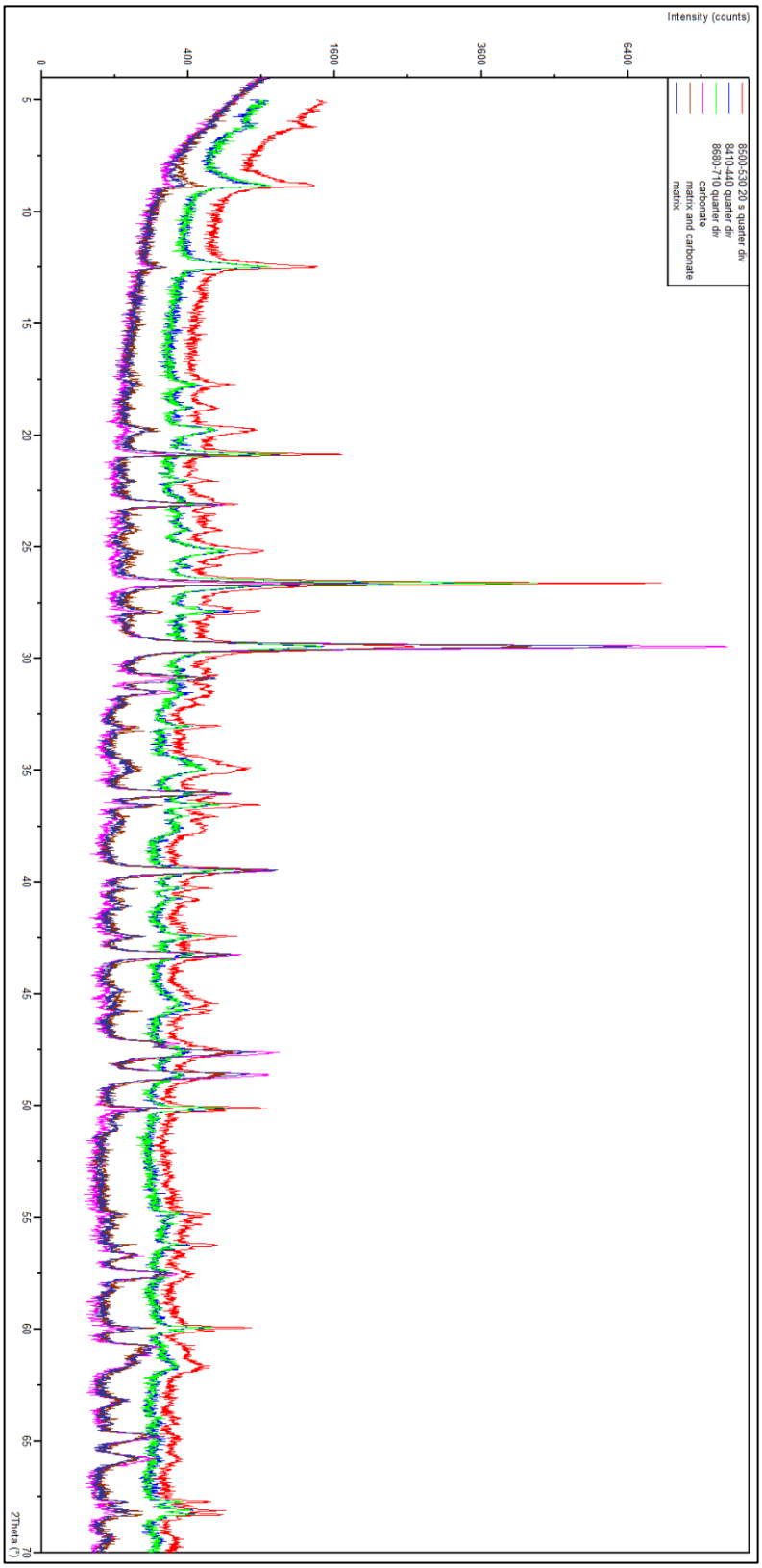

Figure 8B: Combined core and cuttings raw data

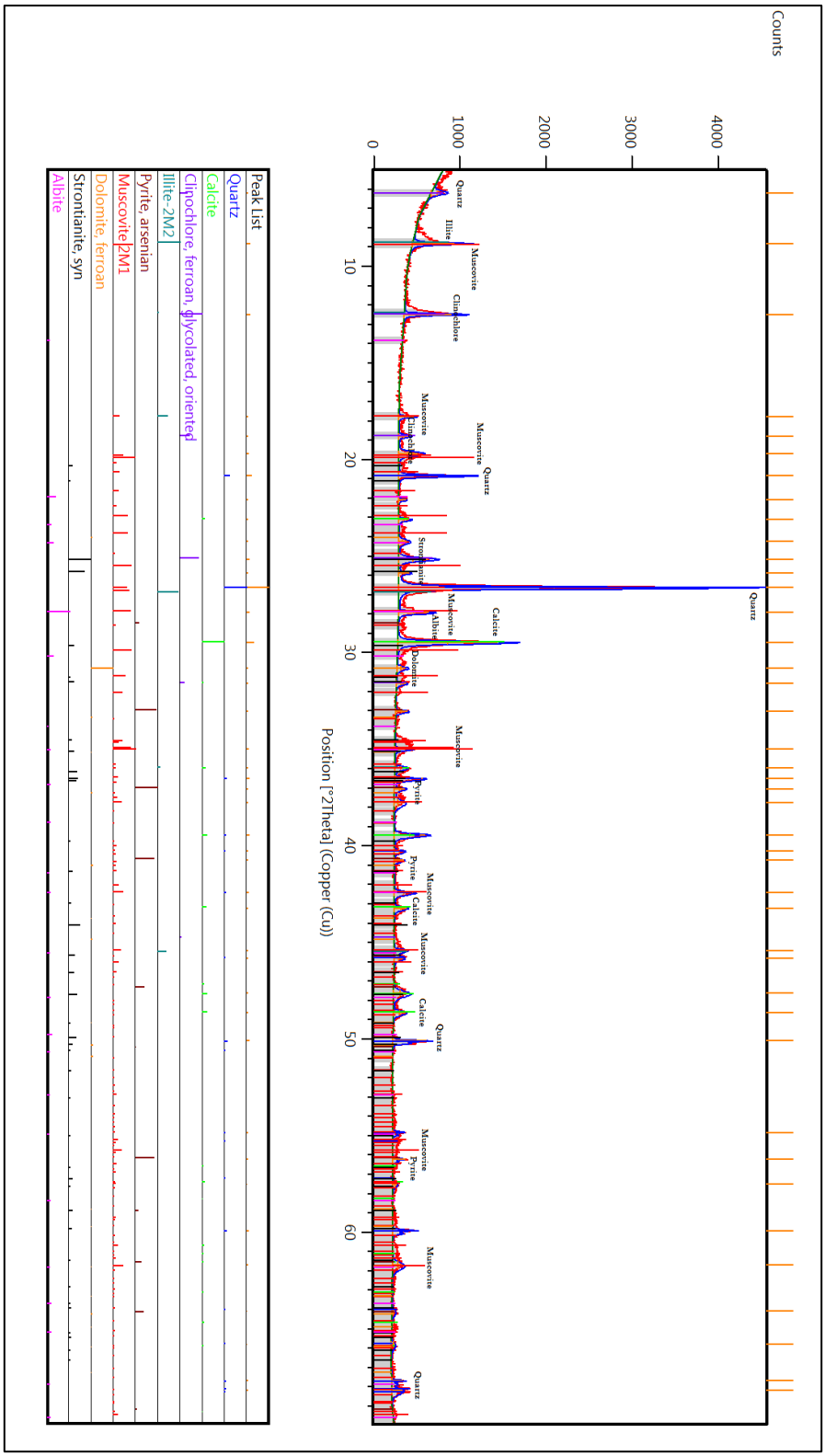

Figure 9B: XRD scan for cuttings depth 8410 ft-8440 ft (one-quarter divergence slit), showing minerals identified

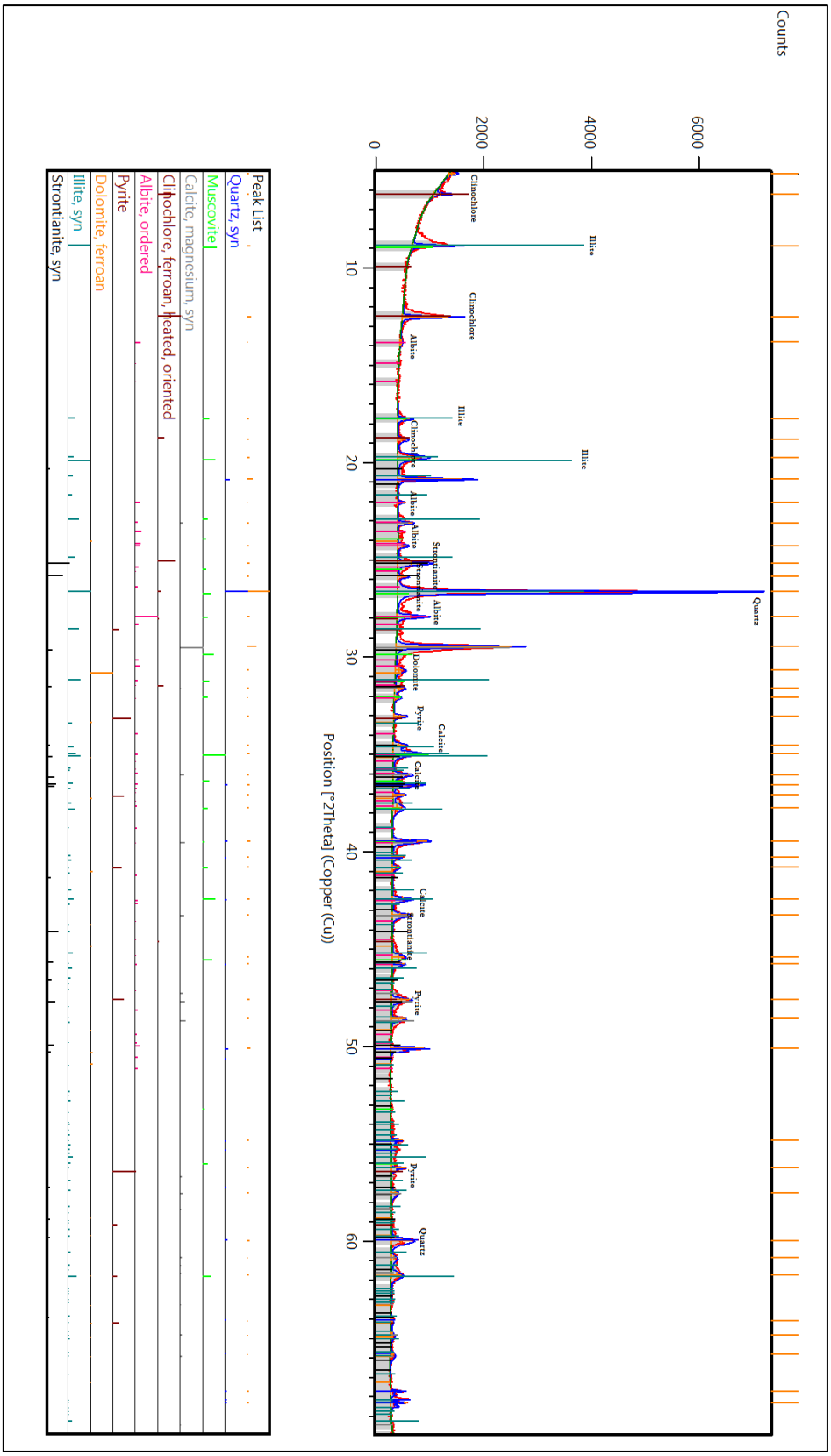

Figure 10B: XRD scan for cuttings depth 8500 ft-8530 ft (20s count time; one-quarter divergence slit)

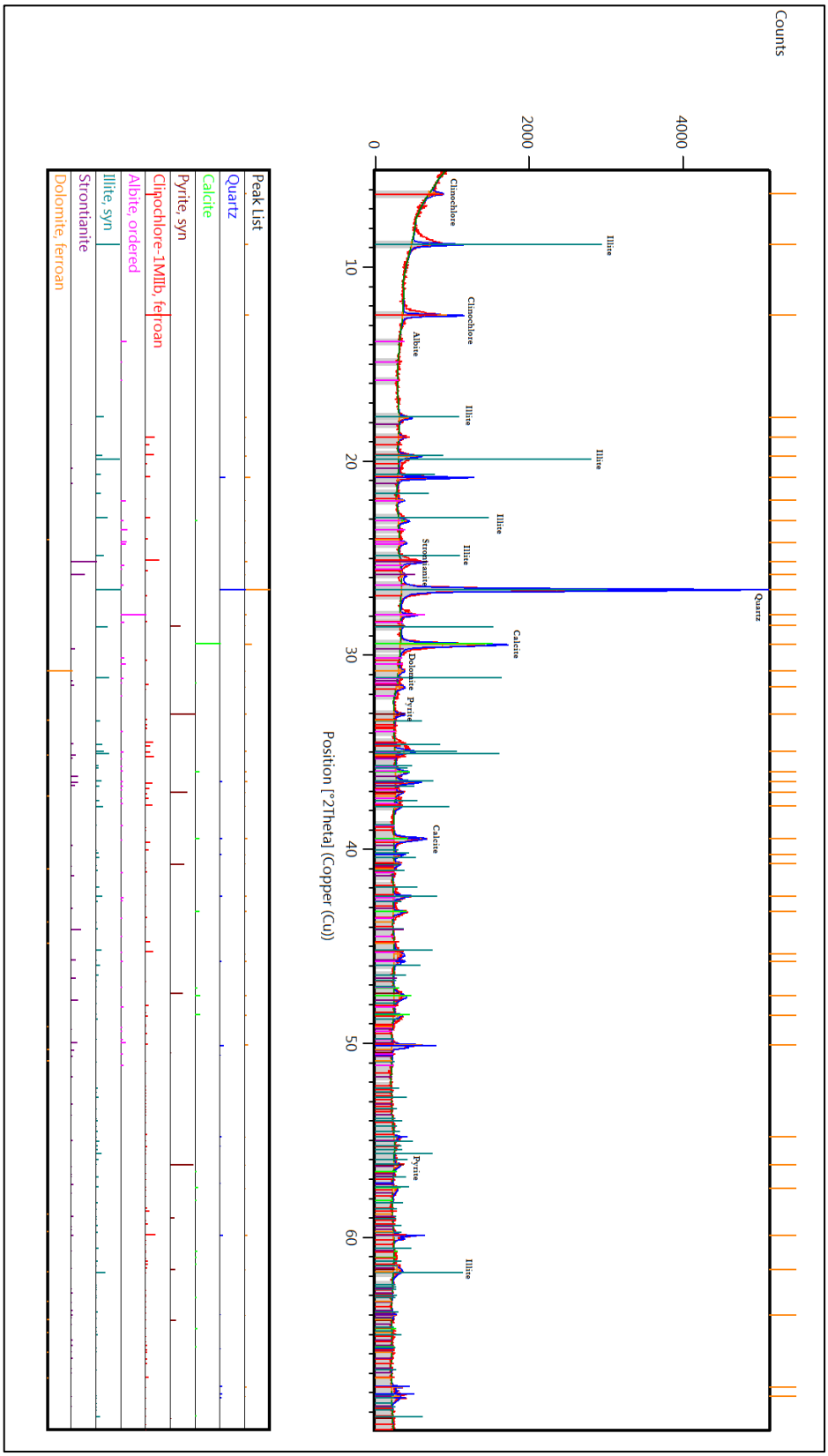

Figure 11B: XRD scan for cuttings depth 8680 ft- 8710 ft (one-quarter divergence slit)

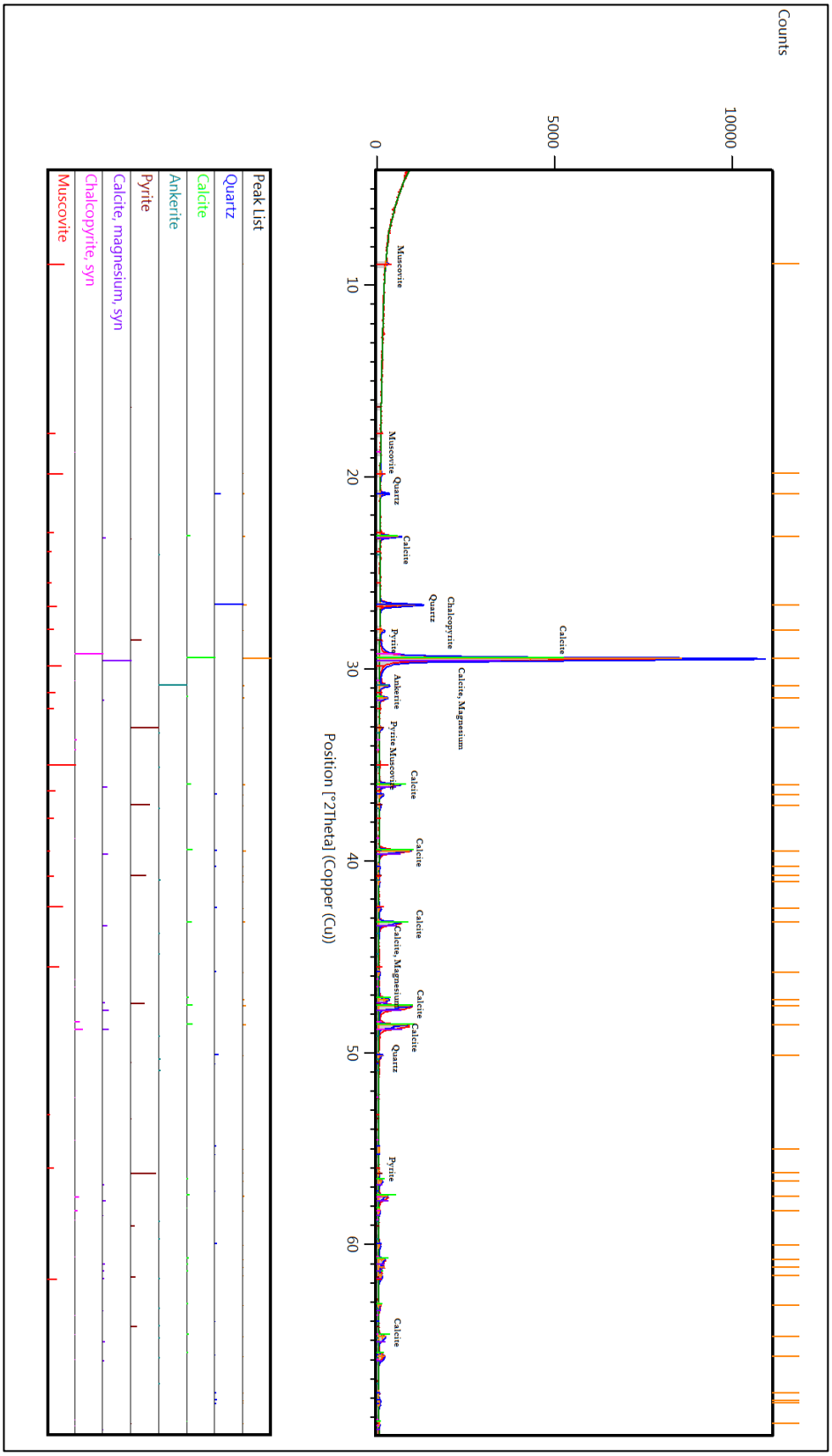

Figure 12B: Core (predominantly carbonate) depth 8479 ft

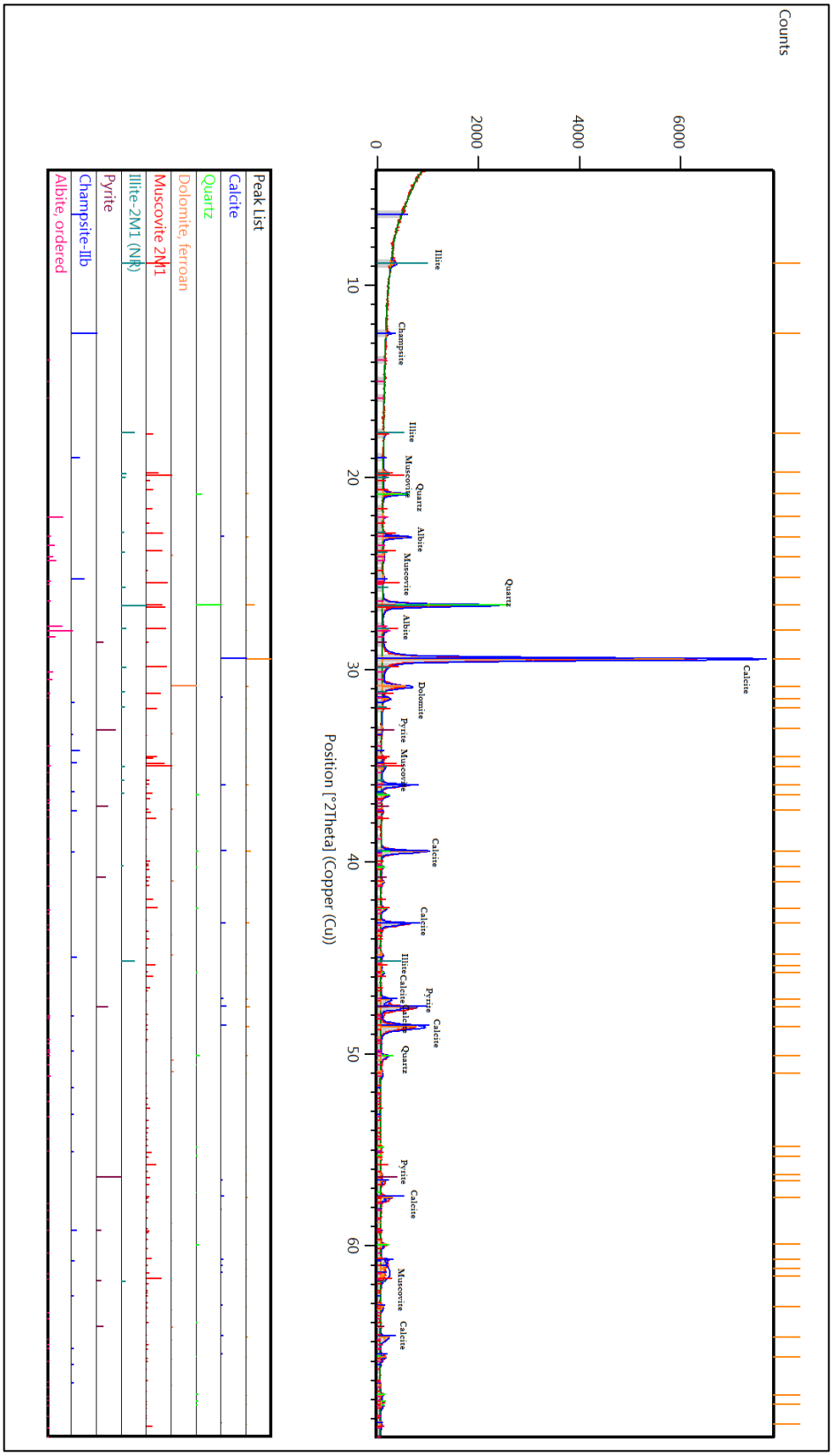

Figure 13B: Core (predominately fine-grained matrix) depth 8479 ft

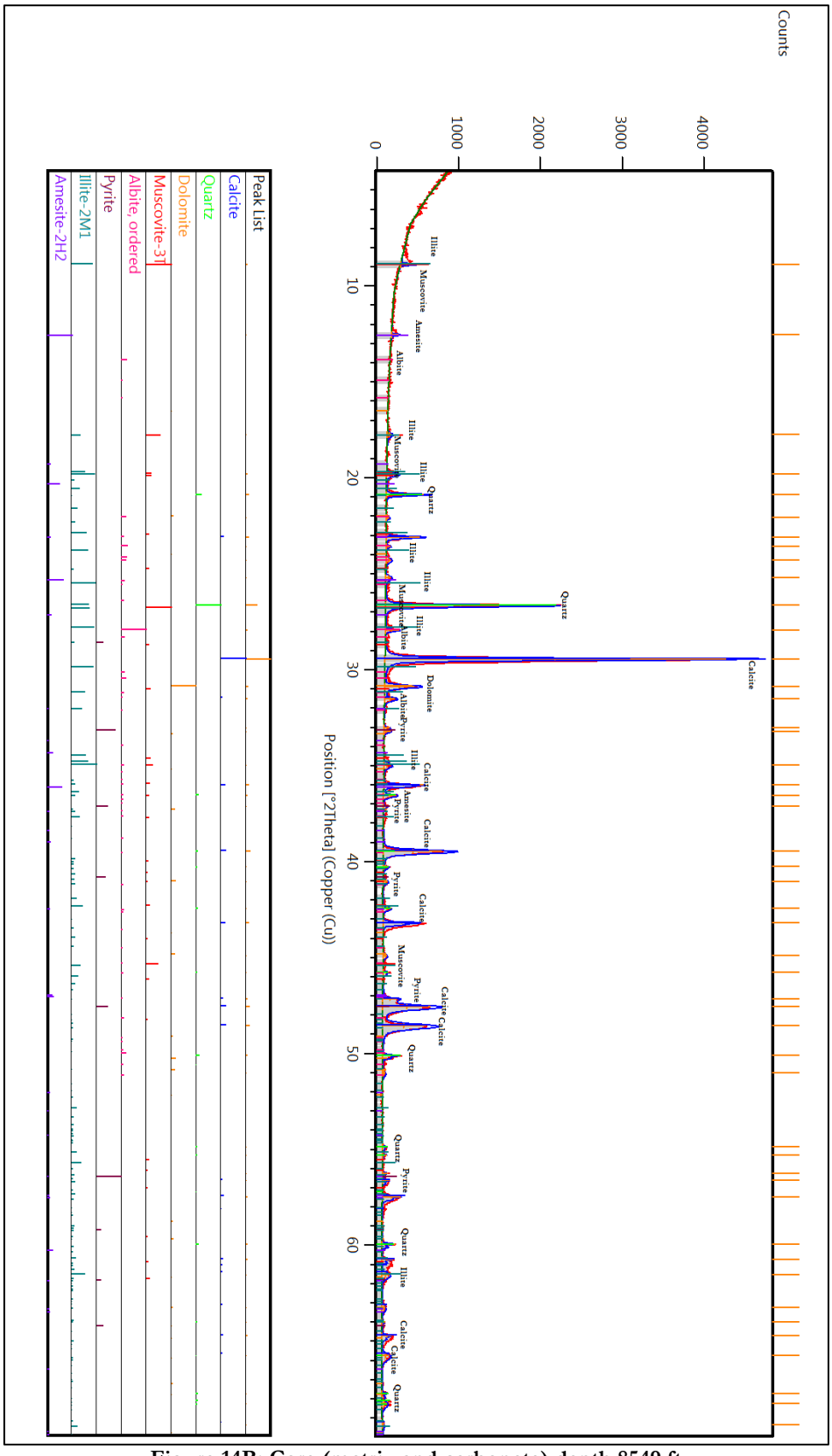

Figure 14B: Core (matrix and carbonate) depth 8549 ft

Appendix C

Sequential Leach Experiments

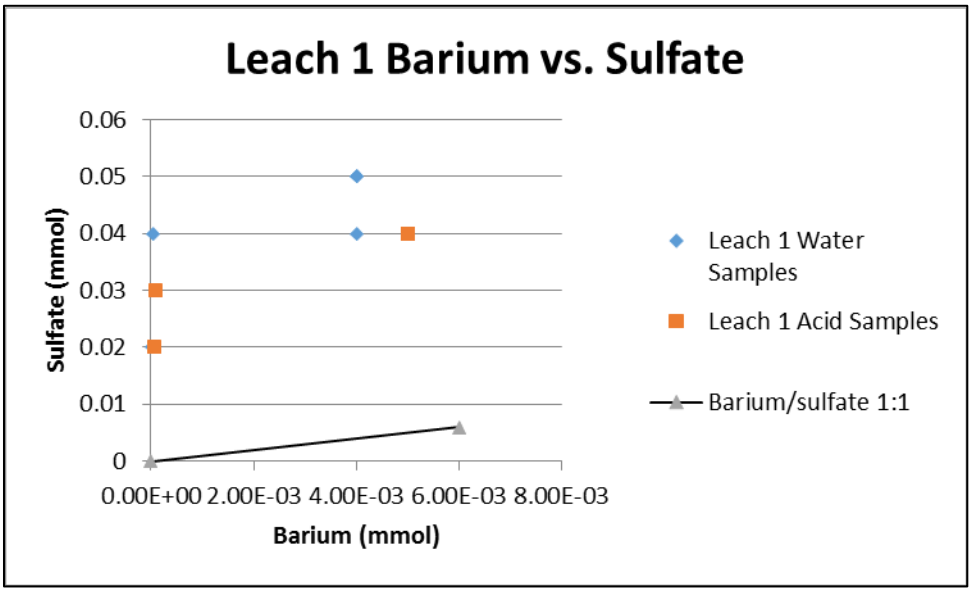

Figure 1C: Barium vs. Sulfate concentrations Leach 1

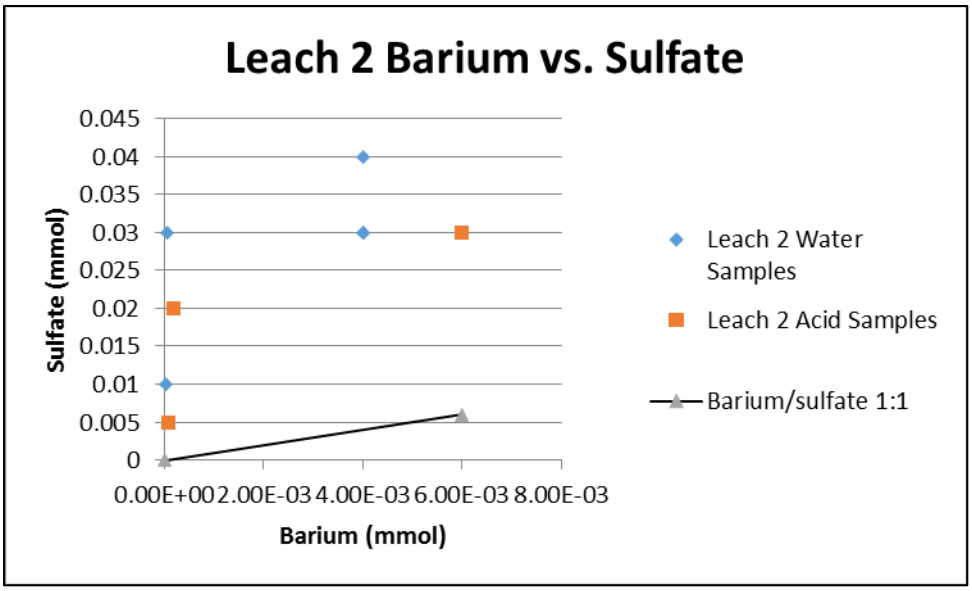

Figure 2C: Barium vs. Sulfate concentrations Leach 2

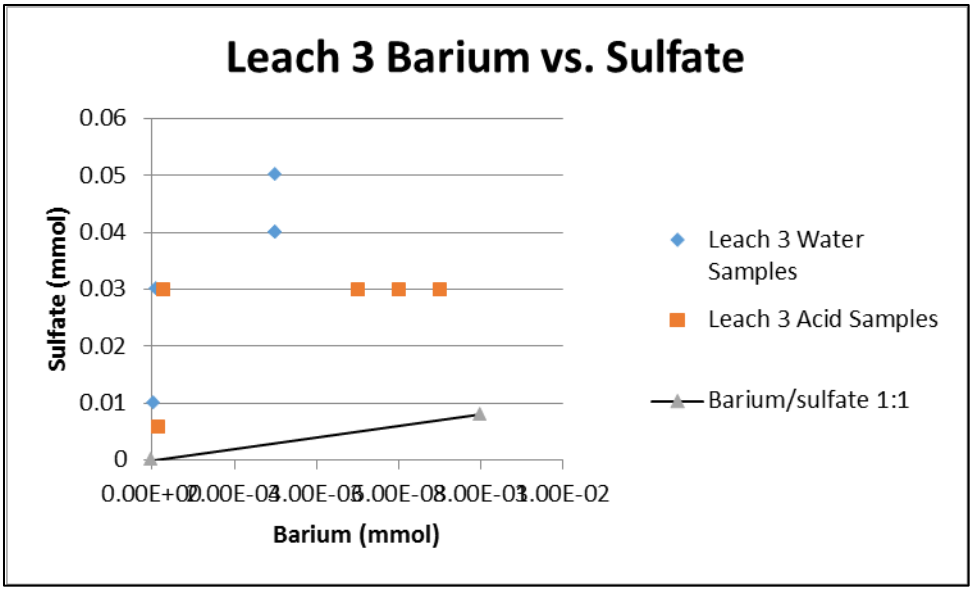

Figure 3C: Barium vs. Sulfate concentrations Leach 3

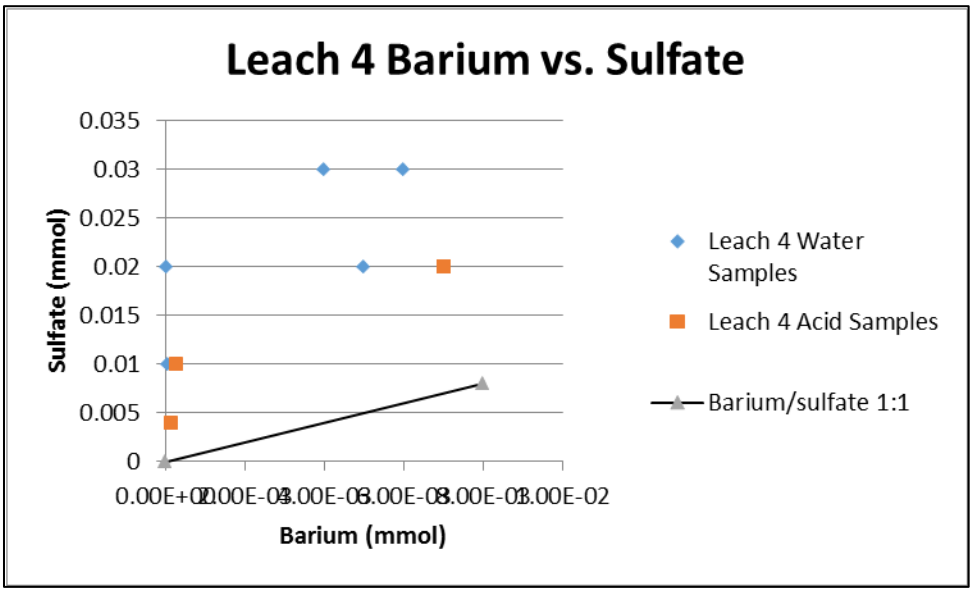

Figure 4C: Barium vs. Sulfate concentrations Leach 4

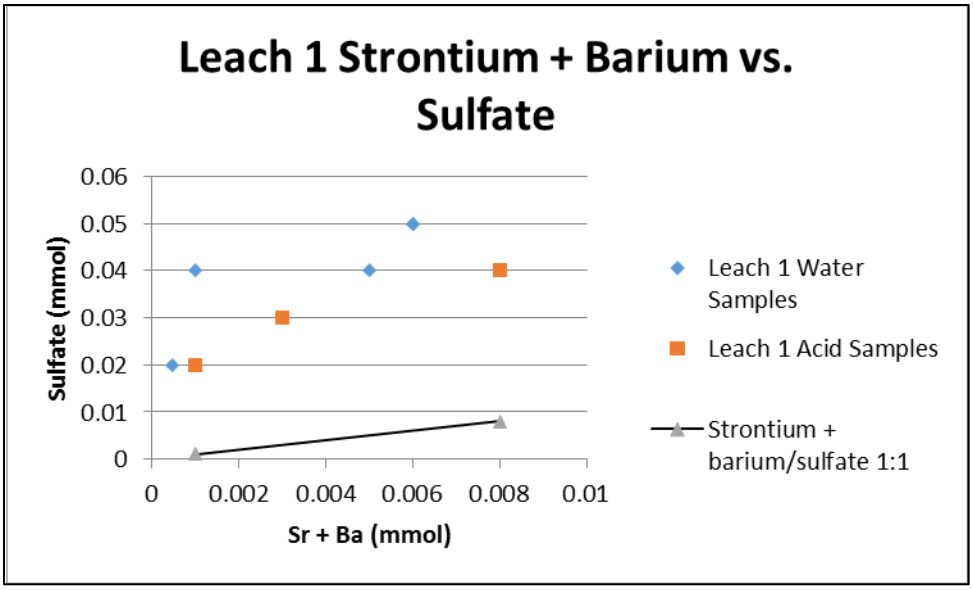

Figure 5C: Strontium + Barium vs. Sulfate concentrations Leach 1

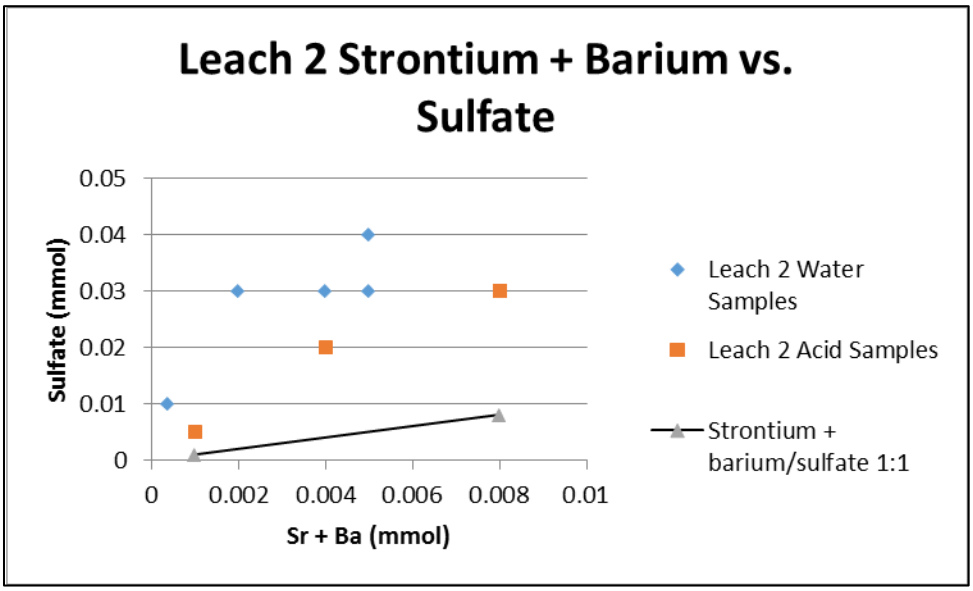

Figure 6C: Strontium + Barium vs. Sulfate concentrations Leach 2

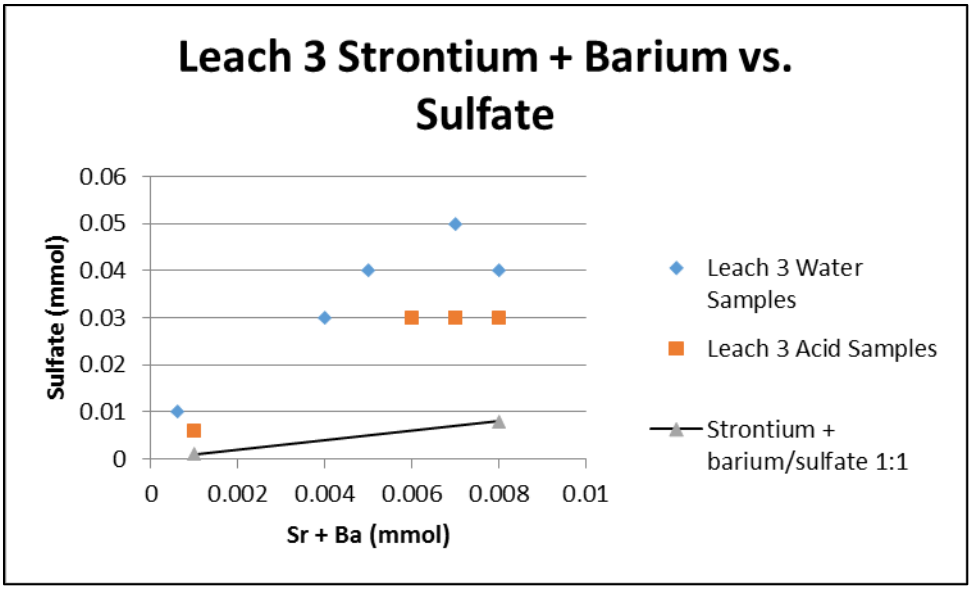

Figure 7C: Strontium + Barium vs. Sulfate concentrations Leach 3

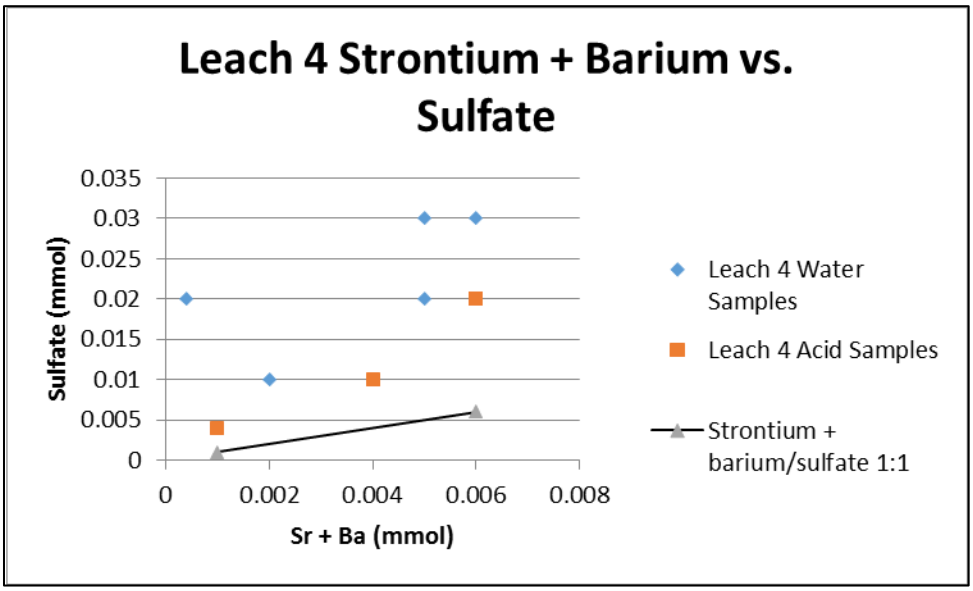

Figure 8C: Strontium + Barium vs. Sulfate concentrations Leach 4

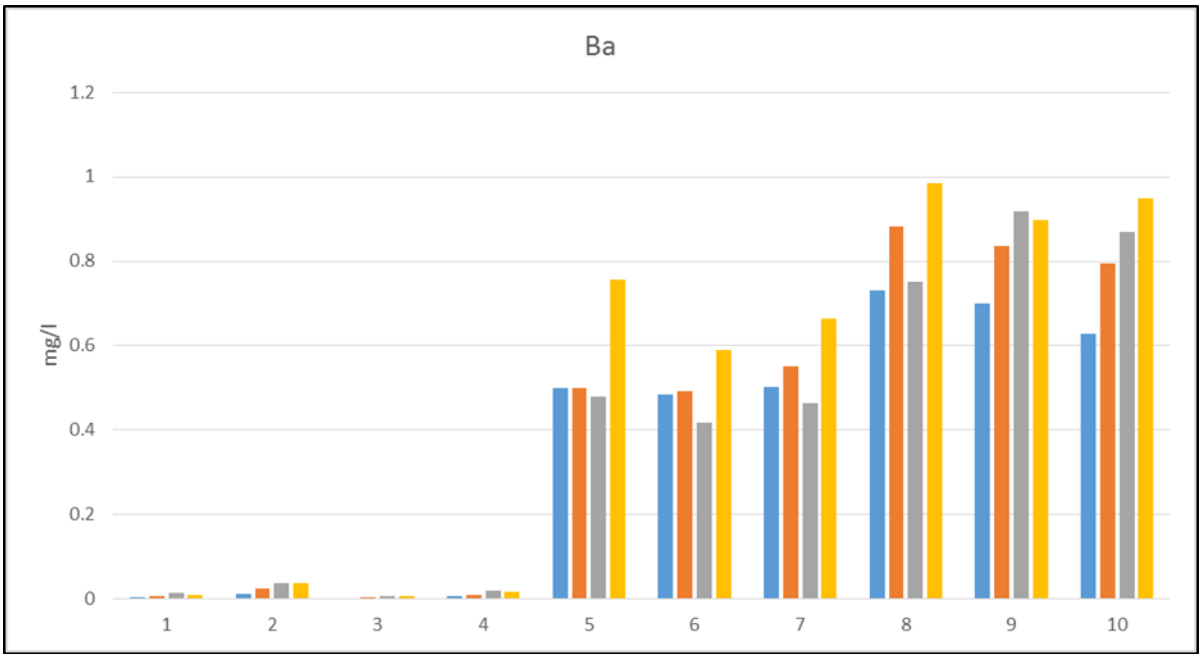

Figure 9C: Barium concentrations M1-M10 Leaches 1-4

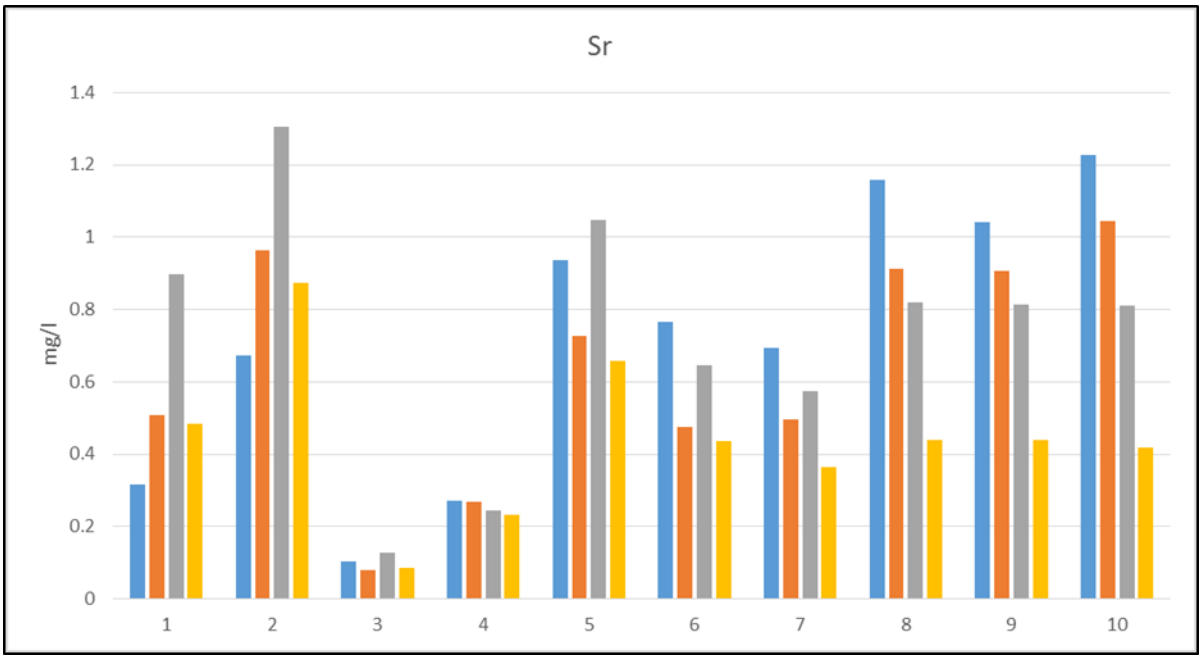

Figure 10C: Strontium concentrations M1-M10 Leaches 1-4

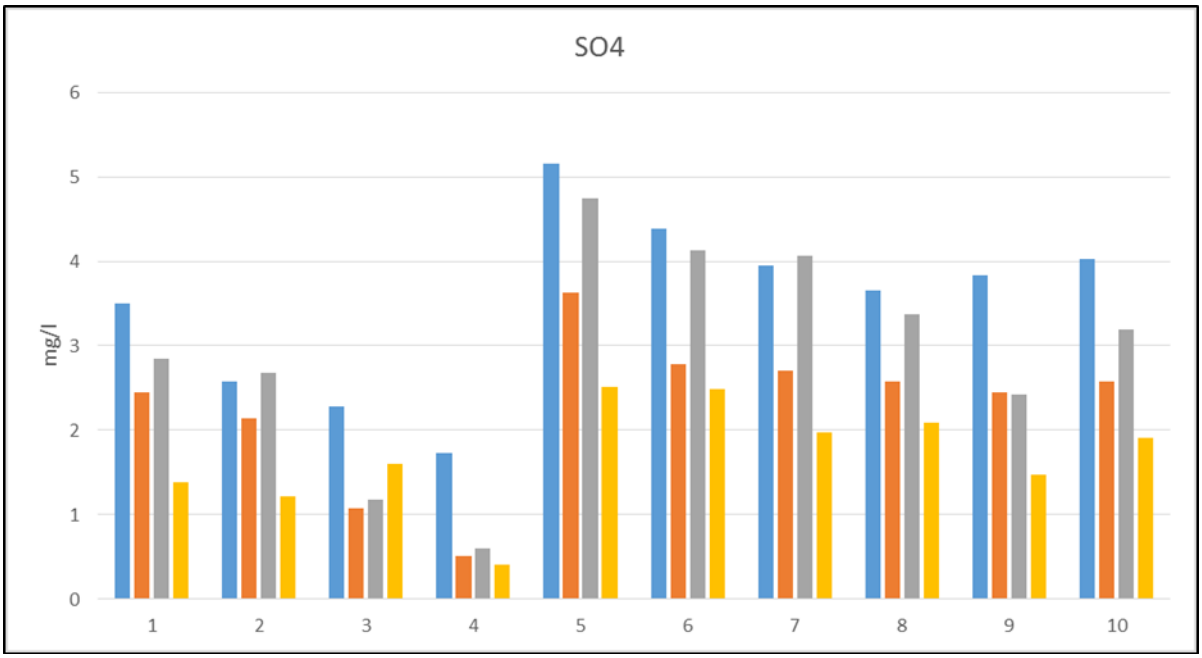

Figure 11C: Sulfate concentrations M1-M10 Leaches 1-4

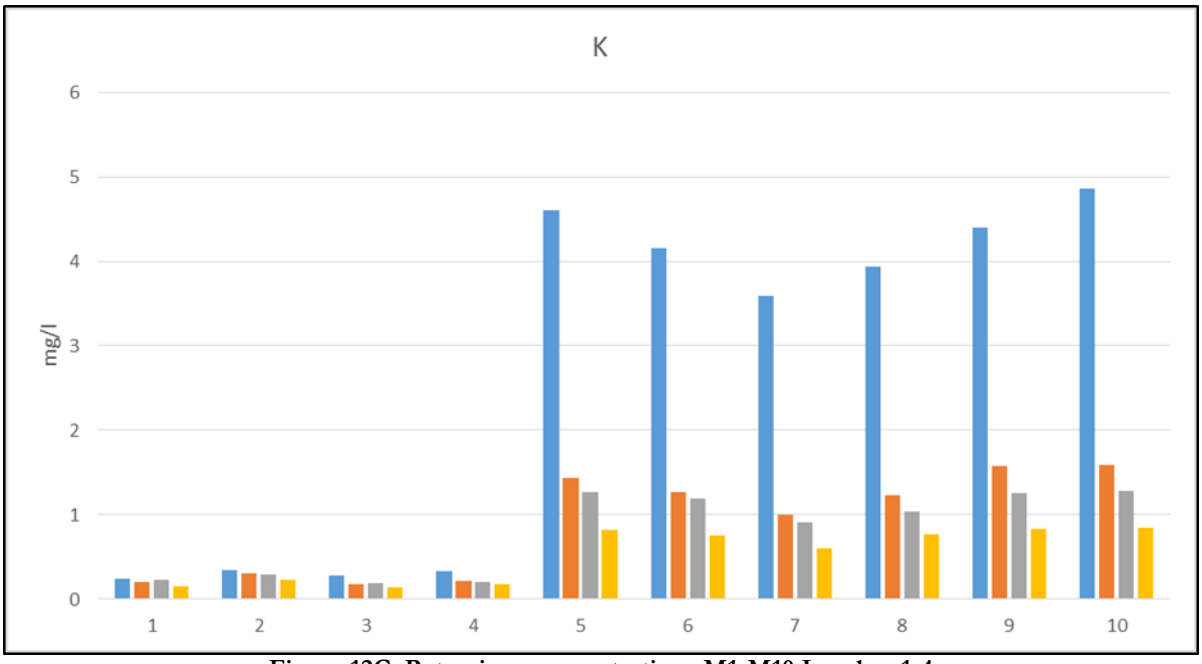

Figure 12C: Potassium concentrations M1-M10 Leaches 1-4

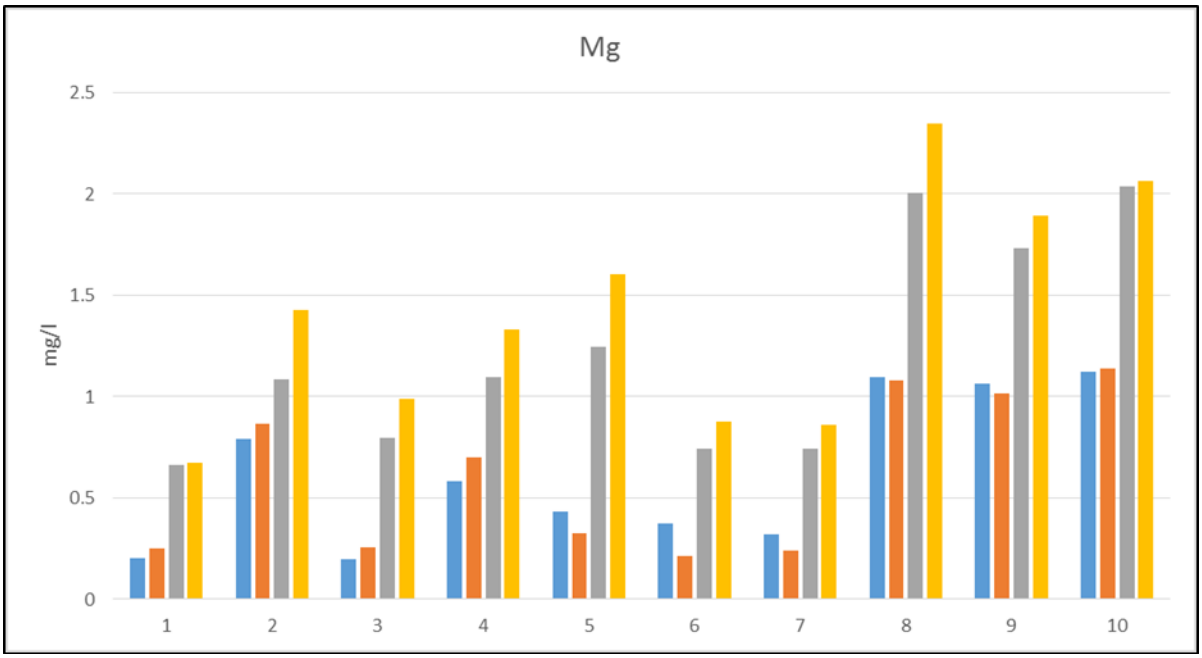

Figure 13C: Magnesium concentrations M1-M10 Leaches 1-4

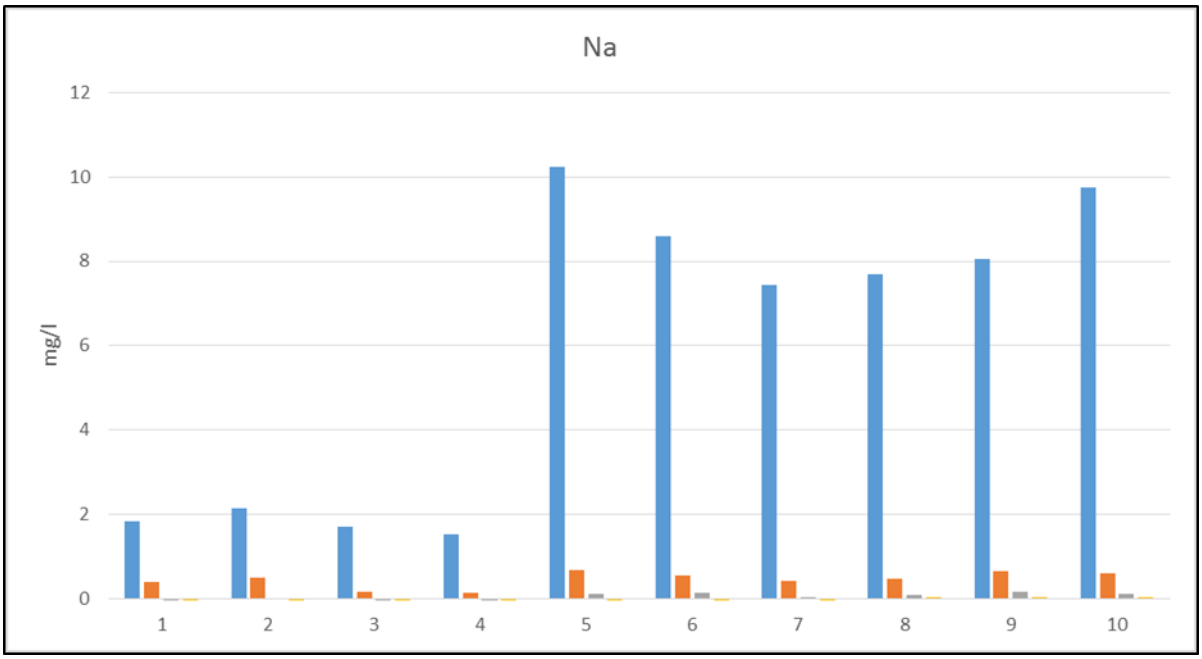

Figure 14C: Sodium concentrations M1-M10 Leaches 1-4

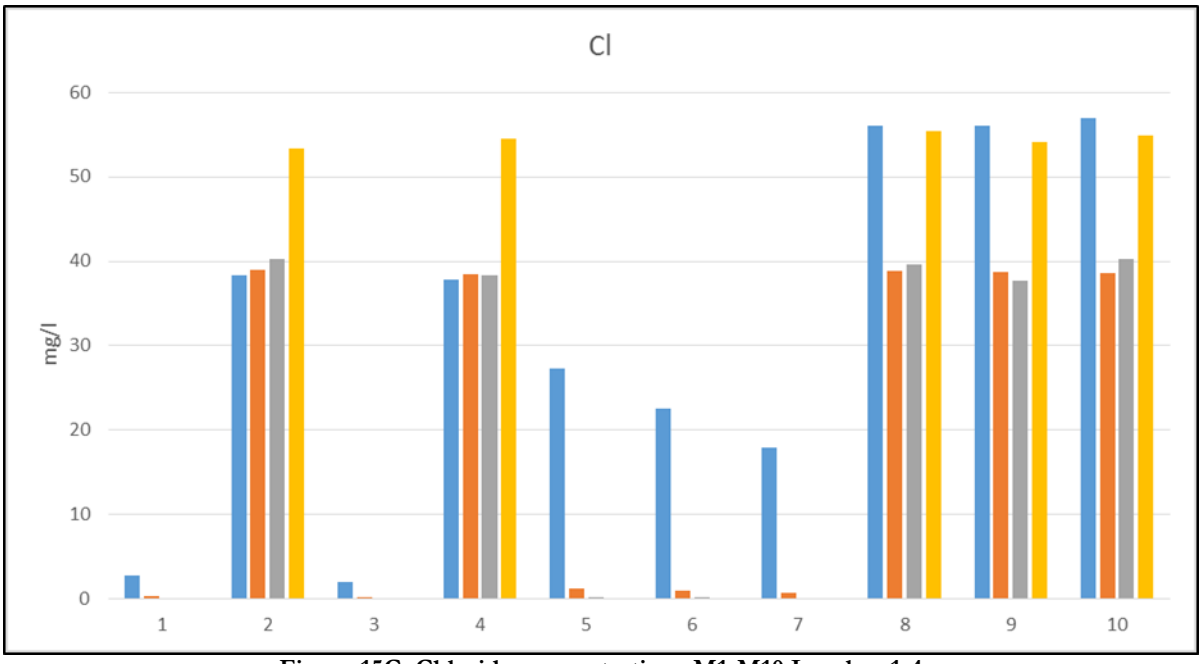

Figure 15C: Chloride concentrations M1-M10 Leaches 1-4

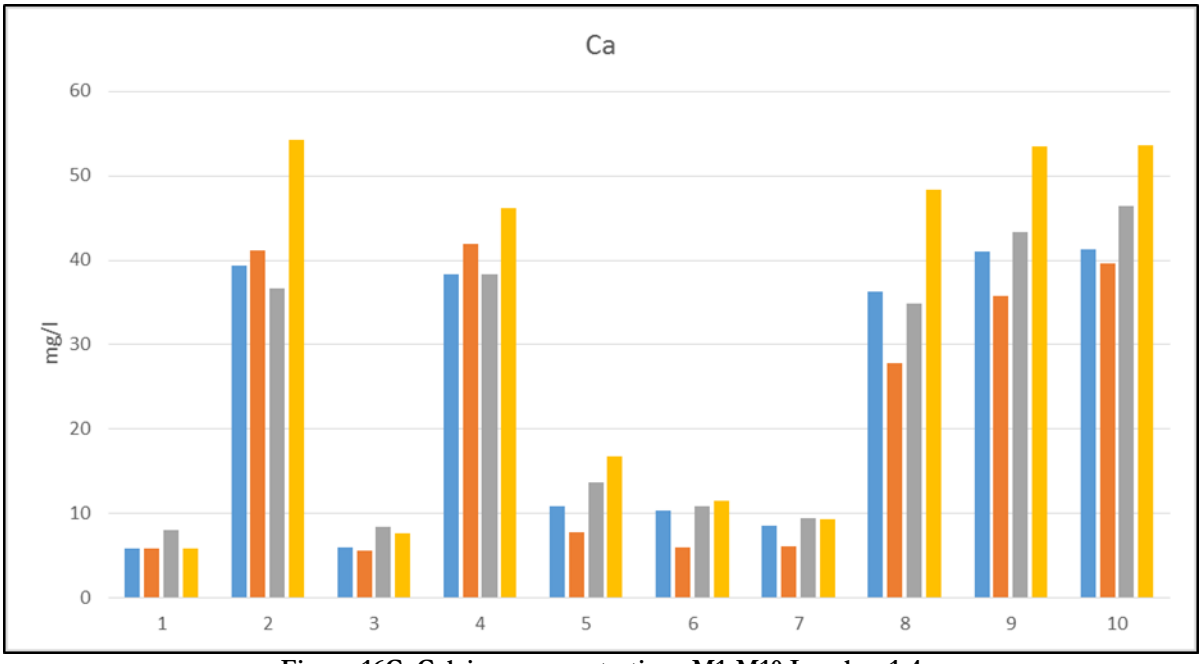

Figure 16C: Calcium concentrations M1-M10 Leaches 1-4

Appendix D

Scanning Electron Microscopy (SEM) and Energy Dispersive X-Ray Spectrometry (EDXS)

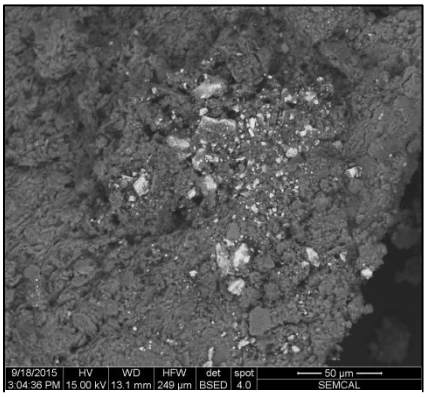

Figure 1D: Cuttings sample leached in acid from depth 8470 ft-8500 ft in the Utica Formation showing a presence of barite represented by the bright grains in the BSED image.

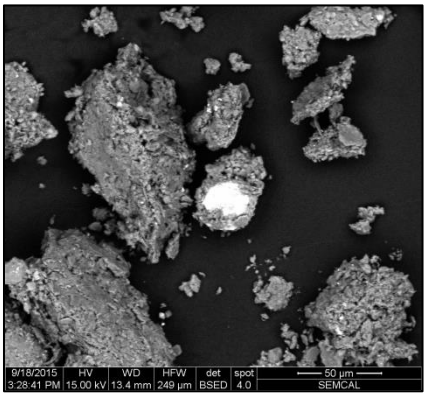

Figure 2D: Cuttings sample leached in acid from depth 8470 ft-8500 ft in the Utica Formation showing a large, euhedral barite grain with smaller grains throughout the BSED image.

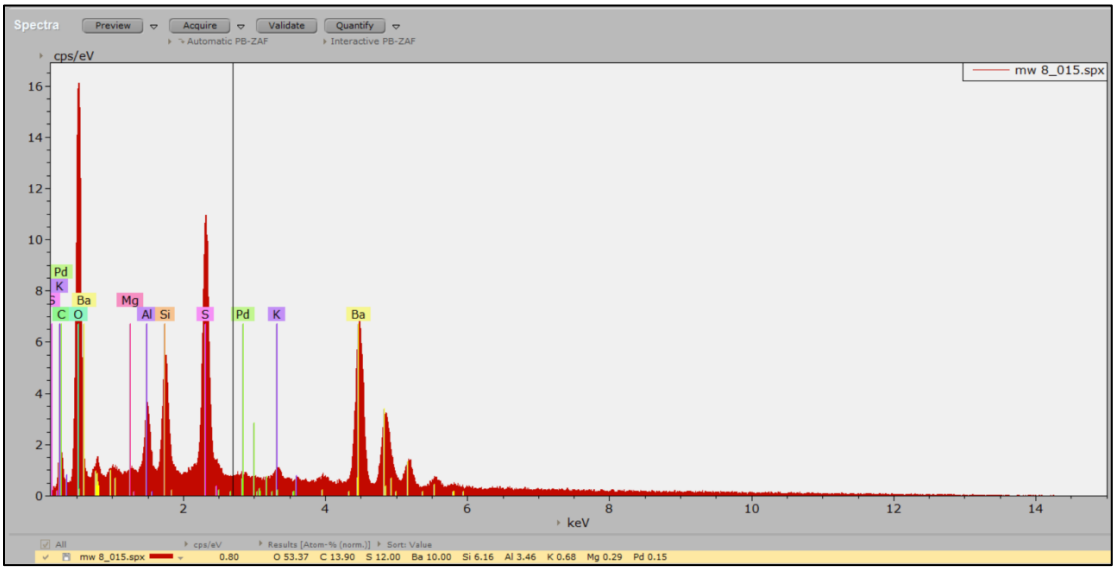

Figure 3D: EDXS data confirming chemistry of cuttings sample leached in acid from depth 8470 ft-8500 ft in the Utica Formation where spot analysis was taken on the large, euhedral grain presented in the BSED image.

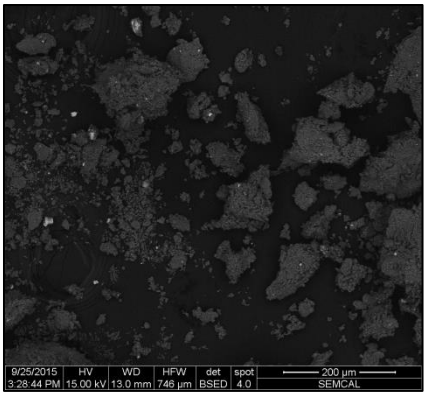

Figure 4D: Cuttings sample leached in water from depth 8470 ft-8500 ft in the Utica Formation showing barite grains throughout the BSED image.

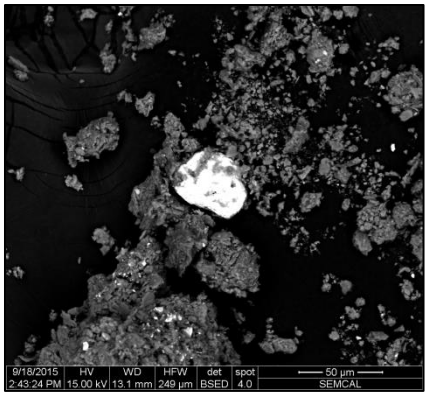

Figure 5D: Cuttings sample leached in water from depth 8500 ft-8530 ft in the Utica Formation showing a large, euhedral barite grain with smaller grains throughout the BSED image.

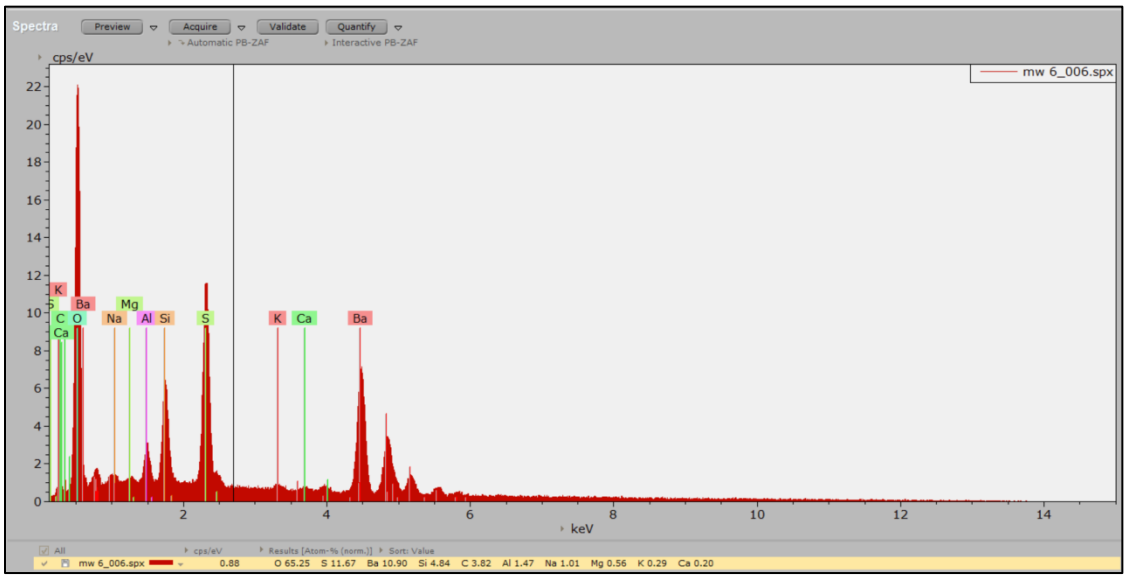

Figure 6D: EDXS data confirming chemistry of cuttings sample leached in water from depth 8500 ft-8530 ft in the Utica Formation where spot analysis was taken on the large, euhedral grain presented in the BSED image.

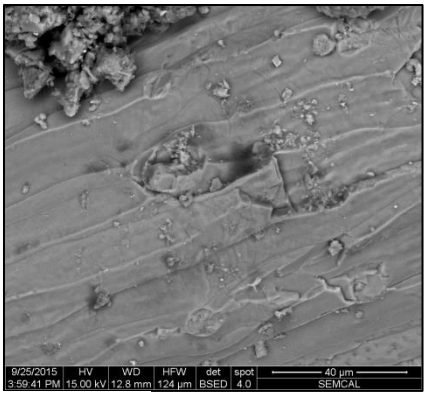

Figure 7D: Core sample leached in acid from depth 8479 ft in the Point Pleasant Formation showing dissolution textures throughout the BSED image.

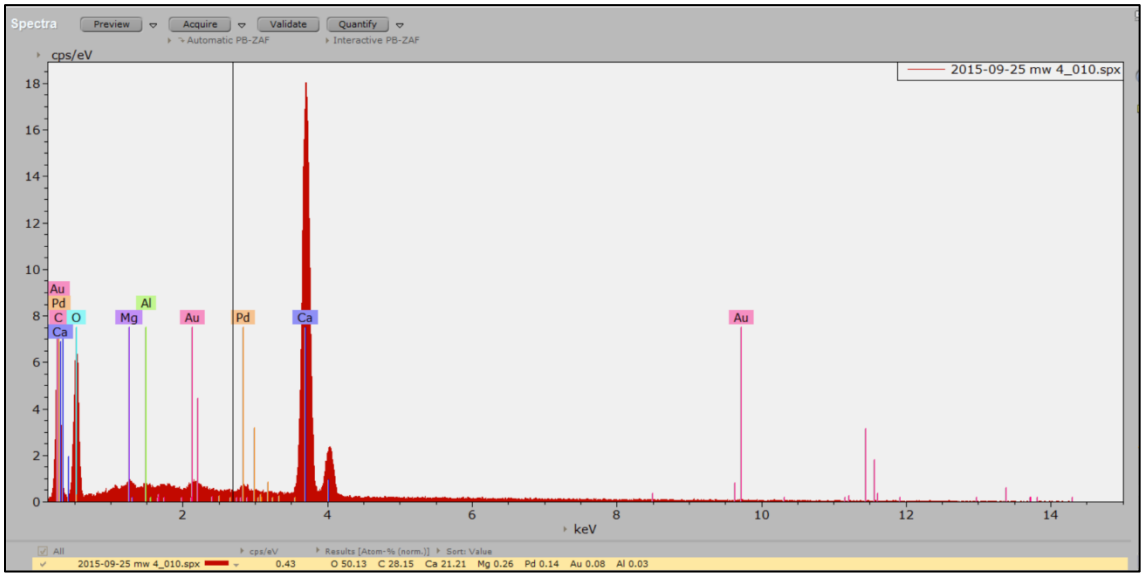

Figure 8D: EDXS data showing calcium carbonate chemistry of core sample leached in acid from depth 8479 ft in the Point Pleasant Formation where spot analysis was taken on the dissolution surface presented in the BSED image.

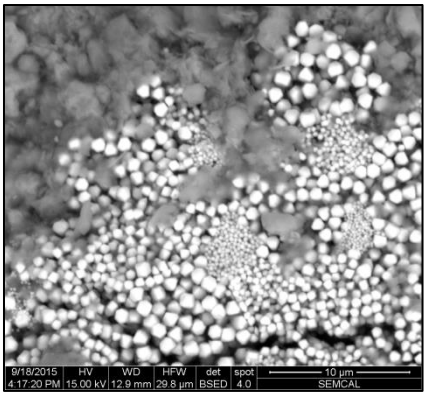

Figure 9D: Core sample leached in acid from depth 8549 ft in the Point Pleasant Formation showing pyrite framboids surrounded by illitic clay throughout the BSED image.

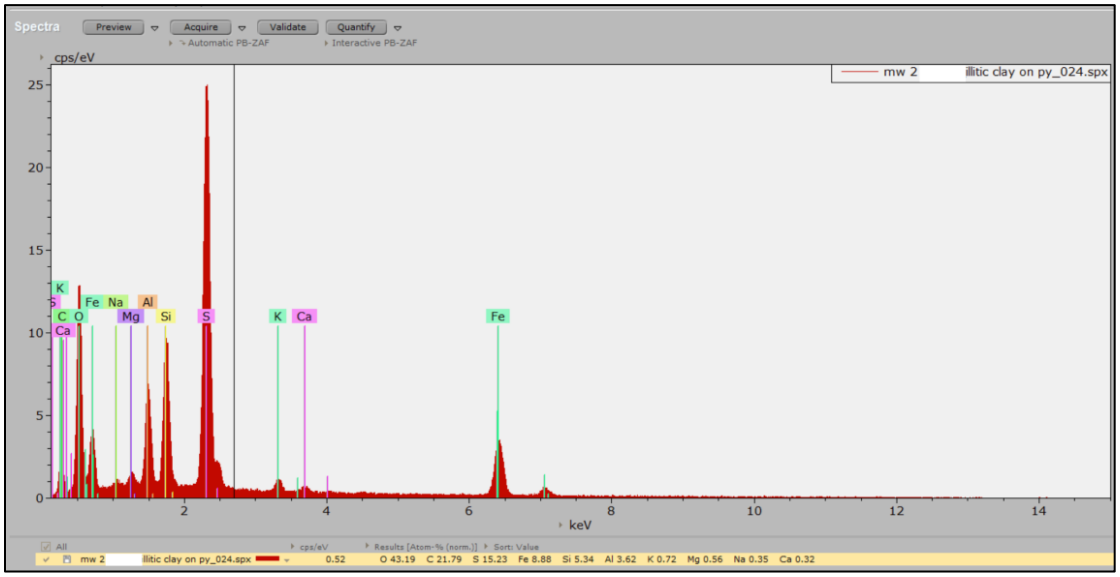

Figure 10: EDXS data confirming pyrite presence in core sample leached in acid from depth 8549 ft in the Point Pleasant Formation where spot analysis was taken on the bright framboids presented in the BSED image.

Appendix E

PHREEQC Geochemical Modeling

Table 1E: Input parameters for Leach 1

F	Cl	Br	N(5)	S(6)	P	Na	Mg	K	Ca	Si	Sr	Ba	Mn(2)	Alkalinity meq/l
0.03	2.73	0.01	0.00	3.50	0.00	1.832	0.202	0.237	5.883	0.111	0.316	0.005	.000001	0.252
0.06	38.38	0.01	0.00	2.58	0.02	2.150	0.790	0.338	39.352	0.101	0.672	0.013	0.023	1.008
0.02	1.97	0.00	0.00	2.27	0.00	1.709	0.193	0.277	5.959	0.120	0.103	0.003	.000001	0.293
0.05	37.87	0.01	0.00	1.73	0.01	1.541	0.582	0.323	38.321	0.091	0.271	0.007	0.025	0.936
0.06	27.28	0.10	0.01	5.16	0.01	10.239	0.429	4.599	10.821	0.431	0.938	0.500	0.001	0.286
0.05	22.50	0.09	0.01	4.39	0.01	8.601	0.370	4.153	10.313	0.379	0.766	0.485	0.000	0.320
0.05	17.91	0.08	0.01	3.95	0.00	7.446	0.321	3.587	8.562	0.499	0.694	0.503	0.000	0.301
0.07	56.04	0.09	0.01	3.65	0.01	7.682	1.094	3.932	36.278	0.305	1.160	0.730	0.096	0.712
0.07	56.10	0.07	0.01	3.83	0.02	8.064	1.062	4.399	41.096	0.265	1.043	0.699	0.109	0.970
0.09	56.92	0.09	0.00	4.03	0.02	9.756	1.124	4.855	41.259	0.387	1.226	0.628	0.088	1.043

Table 2E: Input parameters for Leach 2

F	Cl	Br	N(5)	S(6)	P	Na	Mg	K	Ca	Si	Sr	Ba	Mn(2)	Alkalinity meq/l
0.02	0.38	0.01	0.00	2.44	0.02	0.391	0.249	0.204	5.859	0.138	0.508	0.006	0.00	0.283
0.07	39.00	0.03	0.00	2.13	0.03	0.513	0.864	0.306	41.103	0.134	0.964	0.026	0.023	1.027
0.01	0.18	0.00	0.00	1.07		0.173	0.257	0.174	5.553	0.090	0.080	0.003	0.00	0.284
0.04	38.51	0.01	0.00	0.51	0.01	0.137	0.696	0.212	41.922	0.080	0.267	0.009	0.030	1.069
0.04	1.19	0.02	0.00	3.63	0.01	0.684	0.326	1.427	7.725	0.517	0.727	0.501	0.001	0.390
0.04	0.97	0.00	0.00	2.78	0.00	0.565	0.213	1.265	6.046	0.498	0.475	0.492	0.00	0.307
0.03	0.78	0.01	0.00	2.71	0.01	0.439	0.238	0.999	6.120	0.512	0.496	0.550	0.000	0.308
0.07	38.87	0.00	0.00	2.58	0.01	0.470	1.081	1.234	27.794	0.468	0.911	0.881	0.090	0.409
0.07	38.68	0.00	0.00	2.45	0.01	0.647	1.015	1.571	35.779	0.477	0.906	0.837	0.097	0.826
0.07	38.62	0.04	0.00	2.57	0.01	0.609	1.140	1.591	39.571	0.604	1.046	0.795	0.095	1.025

Table 3E: Input parameters for Leach 3

F	Cl	Br	N(5)	S(6)	P	Na	Mg	K	Ca	Si	Sr	Ba	Mn(2)	Alkalinity meq/l
0.03	0.14	0.00	0.00	2.85	0.00	0.00	0.662	0.232	7.980	0.131	0.897	0.014	0.00	0.415
0.06	40.24	0.00	0.00	2.68	0.06	0.019	1.082	0.285	36.676	0.119	1.303	0.038	0.015	0.764
0.01	0.06	0.00	0.00	1.18	0.00	0.00	0.796	0.194	8.363	0.094	0.127	0.008	0.000	0.464
0.04	38.34	0.02	0.00	0.60	0.02	0.00	1.095	0.204	38.386	0.085	0.244	0.020	0.019	0.921
0.04	0.23	0.01	0.00	4.75	0.00	0.120	1.243	1.263	13.736	1.327	1.047	0.479	0.004	0.748
0.04	0.19	0.00	0.00	4.12	0.00	0.145	0.744	1.186	10.921	1.313	0.646	0.417	0.001	0.570
0.03	0.12	0.01	0.00	4.06	0.01	0.039	0.744	0.905	9.453	1.072	0.573	0.464	0.000	0.488
0.10	39.63	0.03	0.00	3.38	0.02	0.092	2.006	1.039	34.904	1.346	0.820	0.751	0.070	0.774
0.09	37.68	0.00	0.00	2.42	0.00	0.158	1.731	1.248	43.310	1.501	0.815	0.917	0.095	1.258
0.09	40.29	0.00	0.00	3.19	0.00	0.123	2.038	1.274	46.417	1.589	0.810	0.868	0.086	1.347

Table 4E: Input parameters for Leach 4

F	Cl	Br	N(5)	S(6)	P	Na	Mg	K	Ca	Si	Sr	Ba	Mn(2)	Alkalinity meq/l
0.02	0.077	0.006	0.002706075	1.386412243	0.00	0.00	0.662	0.232	7.980	0.131	0.897	0.014	0.00	0.415
0.09	53.373	0.014	0.002324136	1.215517645	0.081741674	0.019	1.082	0.285	36.676	0.119	1.303	0.038	0.015	0.764
0.007	0.052	0.011	0.003065702	1.593882753	0.00	0.00	0.670	0.152	5.880	0.105	0.484	0.009	0.00	0.332
0.047	54.545	0.013	0.002667737	0.405221064	0.039133136	0.00	1.424	0.225	54.243	0.077	0.874	0.037	0.031	1.315
0.030	0.078	0.006	0.002499827	2.513219809	0.00	0.00	0.987	0.133	7.609	0.074	0.086	0.006	0.00	0.431
0.033	0.102	0.006		2.480501115	0.00	0.00	1.331	0.171	46.121	0.069	0.232	0.018	0.025	0.872
0.015	0.077	0.010	0.003416619	1.97620701	0.00118786	0.00	1.604	0.813	16.732	1.126	0.658	0.757	0.011	0.957
0.079	55.403	0.024		2.092741176	0.019787704	0.00	0.878	0.751	11.503	1.163	0.436	0.588	0.002	0.628
0.115	54.117	0.00		1.466513235	0.03281306	0.00	0.858	0.595	9.303	0.875	0.365	0.664	0.001	0.524
0.113	54.836	0.002	0.001733565	1.902711085	0.029328454	0.041	2.345	0.767	48.351	1.255	0.438	0.984	0.107	1.042
						0.048	1.889	0.831	53.428	1.582	0.439	0.899	0.114	1.306
						0.037	2.062	0.843	53.587	1.397	0.420	0.948	0.110	1.299

Table 5E: Saturation indices
MW1 Leach 1

MW 1 Leach 1	
Phase:	Saturation Index:
Aragonite	-2.49
Calcite	-2.35
Dolomite	-5.81
Barite	-2.02
Celestite	-3.33
Gypsum	-3.8
Strontianite	-3.16

Table 6E: Saturation indices
MW2 Leach 1

MW 2 Leach 1	
Phase:	Saturation Index:
Aragonite	-1.14
Calcite	-1
Dolomite	-3.34
Barite	-1.89
Celestite	-3.29
Gypsum	-3.26
Strontianite	-2.31

Table 7E: Saturation indices
MW3 Leach 1

MW 3 Leach 1	
Phase:	Saturation Index:
Aragonite	-2.42
Calcite	-2.27
Dolomite	-5.69
Barite	-2.43
Celestite	-4.01
Gypsum	-3.98
Strontianite	-3.58

Table 8E: Saturation indices
MW4 Leach 1

MW 4 Leach 1	
Phase:	Saturation Index:
Aragonite	-1.18
Calcite	-1.04
Dolomite	-3.54
Barite	-2.32
Celestite	-3.85
Gypsum	-3.44
Strontianite	-2.74

Table 9E: Saturation indices
MW5 Leach 1

MW 5 Leach 1	
Phase:	Saturation Index:
Aragonite	-2.2
Calcite	-2.06
Dolomite	-5.18
Barite	0.09
Celestite	-2.75
Gypsum	-3.43
Strontianite	-2.67

Table 10E: Saturation indices
MW6 Leach 1

MW 6 Leach 1	
Phase:	Saturation Index:
Aragonite	-2.17
Calcite	-2.03
Dolomite	-5.15
Barite	0.01
Celestite	-2.9
Gypsum	-3.51
Strontianite	-2.71

Table 11E: Saturation indices
MW7 Leach 1

MW 7 Leach 1	
Phase:	Saturation Index:
Aragonite	-2.27
Calcite	-2.13
Dolomite	-5.34
Barite	-0.01
Celestite	-2.98
Gypsum	-3.63
Strontianite	-2.77

Table 12E: Saturation indices
MW8 Leach 1

MW 8 Leach 1	
Phase:	Saturation Index:
Aragonite	-1.33
Calcite	-1.18
Dolomite	-3.54
Barite	0.01
Celestite	-2.91
Gypsum	-3.15
Strontianite	-2.23

Table 13E: Saturation indices
MW9 Leach 1

MW 9 Leach 1	
Phase:	Saturation Index:
Aragonite	-1.15
Calcite	-1
Dolomite	-3.25
Barite	-0.01
Celestite	-2.95
Gypsum	-3.09
Strontianite	-2.15

Table 14E: Saturation indices
MW10 Leach 1

MW 10 Leach 1	
Phase:	Saturation Index:
Aragonite	-1.12
Calcite	-0.97
Dolomite	-3.16
Barite	-0.03
Celestite	-2.86
Gypsum	-3.07
Strontianite	-2.05

Table 15E: Saturation indices
MW1 Leach 2

MW 1 Leach 2	
Phase:	Saturation Index:
Aragonite	-2.44
Calcite	-2.29
Dolomite	-5.61
Barite	-2.09
Celestite	-3.28
Gypsum	-3.95
Strontianite	-2.9

Table 16E: Saturation indices
MW2 Leach 2

MW 2 Leach 2	
Phase:	Saturation Index:
Aragonite	-1.11
Calcite	-0.97
Dolomite	-3.27
Barite	-1.67
Celestite	-3.22
Gypsum	-3.33
Strontianite	-2.15

Table 17E: Saturation indices
MW3 Leach 2

MW 3 Leach 2	
Phase:	Saturation Index:
Aragonite	-2.45
Calcite	-2.31
Dolomite	-5.61
Barite	-2.74
Celestite	-4.43
Gypsum	-4.33
Strontianite	-3.7

Table 18E: Saturation indices
MW4 Leach 2

MW 4 Leach 2	
Phase:	Saturation Index:
Aragonite	-1.09
Calcite	-0.94
Dolomite	-3.32
Barite	-2.75
Celestite	-4.4
Gypsum	-3.94
Strontianite	-2.69

Table 19E: Saturation indices
MW5 Leach 2

MW 5 Leach 2	
Phase:	Saturation Index:
Aragonite	-2.19
Calcite	-2.05
Dolomite	-5.12
Barite	-0.02
Celestite	-2.97
Gypsum	-3.68
Strontianite	-2.62

Table 20E: Saturation indices
MW6 Leach 2

MW 6 Leach 2	
Phase:	Saturation Index:
Aragonite	-2.39
Calcite	-2.25
Dolomite	-5.6
Barite	-0.13
Celestite	-3.26
Gypsum	-3.89
Strontianite	-2.9

Table 21E: Saturation indices
MW7 Leach 2

MW 7 Leach 2	
Phase:	Saturation Index:
Aragonite	-2.38
Calcite	-2.24
Dolomite	-5.54
Barite	-0.09
Celestite	-3.25
Gypsum	-3.89
Strontianite	-2.88

Table 22E: Saturation indices
MW8 Leach 2

MW 8 Leach 2	
Phase:	Saturation Index:
Aragonite	-1.66
Calcite	-1.52
Dolomite	-4.1
Barite	-0.02
Celestite	-3.12
Gypsum	-3.37
Strontianite	-2.55

Table 23E: Saturation indices
MW9 Leach 2

MW 9 Leach 2	
Phase:	Saturation Index:
Aragonite	-1.26
Calcite	-1.12
Dolomite	-3.43
Barite	-0.09
Celestite	-3.17
Gypsum	-3.31
Strontianite	-2.26

Table 24E: Saturation indices
MW10 Leach 2

MW 10 Leach 2	
Phase:	Saturation Index:
Aragonite	-1.13
Calcite	-0.99
Dolomite	-3.17
Barite	-0.11
Celestite	-3.1
Gypsum	-3.26
Strontianite	-2.11

Table 25E: Saturation indices
MW1 Leach 3

MW 1 Leach 3	
Phase:	Saturation Index:
Aragonite	-2.15
Calcite	-2
Dolomite	-4.74
Barite	-1.68
Celestite	-2.98
Gypsum	-3.77
Strontianite	-2.5

Table 26E: Saturation indices
MW2 Leach 3

MW 2 Leach 3	
Phase:	Saturation Index:
Aragonite	-1.28
Calcite	-1.14
Dolomite	-3.46
Barite	-1.4
Celestite	-2.98
Gypsum	-3.26
Strontianite	-2.14

Table 27E: Saturation indices
MW3 Leach 3

MW 3 Leach 3	
Phase:	Saturation Index:
Aragonite	-2.08
Calcite	-1.93
Dolomite	-4.54
Barite	-2.3
Celestite	-4.22
Gypsum	-4.13
Strontianite	-3.3

Table 28E: Saturation indices
MW4 Leach 3

MW 4 Leach 3	
Phase:	Saturation Index:
Aragonite	-1.18
Calcite	-1.04
Dolomite	-3.28
Barite	-2.33
Celestite	-4.36
Gypsum	-3.9
Strontianite	-2.79

Table 29E: Saturation indices
MW5 Leach 3

MW 5 Leach 3	
Phase:	Saturation Index:
Aragonite	-1.68
Calcite	-1.54
Dolomite	-3.77
Barite	0.03
Celestite	-2.74
Gypsum	-3.36
Strontianite	-2.2

Table 30E: Saturation indices
MW6 Leach 3

MW 6 Leach 3	
Phase:	Saturation Index:
Aragonite	-1.89
Calcite	-1.74
Dolomite	-4.3
Barite	-0.07
Celestite	-2.99
Gypsum	-3.5
Strontianite	-2.52

Table 31E: Saturation indices
MW7 Leach 3

MW 7 Leach 3	
Phase:	Saturation Index:
Aragonite	-2.01
Calcite	-1.87
Dolomite	-4.49
Barite	-0.02
Celestite	-3.04
Gypsum	-3.56
Strontianite	-2.63

Table 32E: Saturation indices
MW8 Leach 3

MW 8 Leach 3	
Phase:	Saturation Index:
Aragonite	-1.3
Calcite	-1.16
Dolomite	-3.21
Barite	0
Celestite	-3.08
Gypsum	-3.19
Strontianite	-2.34

Table 33E: Saturation indices
MW9 Leach 3

MW 9 Leach 3	
Phase:	Saturation Index:
Aragonite	-1.01
Calcite	-0.87
Dolomite	-2.78
Barite	-0.09
Celestite	-3.25
Gypsum	-3.26
Strontianite	-2.14

Table 34E: Saturation indices
MW10 Leach 3

MW 10 Leach 3	
Phase:	Saturation Index:
Aragonite	-0.96
Calcite	-0.81
Dolomite	-2.63
Barite	0
Celestite	-3.15
Gypsum	-3.12
Strontianite	-2.12

Table 35E: Saturation indices
MW1 Leach 4

MW 1 Leach 4	
Phase:	Saturation Index:
Aragonite	-2.15
Calcite	-2
Dolomite	-4.74
Barite	-1.99
Celestite	-3.29
Gypsum	-4.08
Strontianite	-2.5

Table 36E: Saturation indices
MW2 Leach 4

MW 2 Leach 4	
Phase:	Saturation Index:
Aragonite	-1.29
Calcite	-1.14
Dolomite	-3.47
Barite	-1.74
Celestite	-3.32
Gypsum	-3.61
Strontianite	-2.14

Table 37E: Saturation indices
MW3 Leach 4

MW 3 Leach 4	
Phase:	Saturation Index:
Aragonite	-2.37
Calcite	-2.22
Dolomite	-5.04
Barite	-2.1
Celestite	-3.49
Gypsum	-4.14
Strontianite	-2.86

Table 38E: Saturation indices
MW4 Leach 4

MW 4 Leach 4	
Phase:	Saturation Index:
Aragonite	-0.9
Calcite	-0.76
Dolomite	-2.75
Barite	-2.28
Celestite	-4.02
Gypsum	-3.97
Strontianite	-2.1

Table 39E: Saturation indices
MW5 Leach 4

MW 5 Leach4	
Phase:	Saturation Index:
Aragonite	-2.15
Calcite	-2.1
Dolomite	-4.55
Barite	-2.1
Celestite	-4.06
Gypsum	-3.85
Strontianite	-3.5

Table 40E: Saturation indices
MW6 Leach 4

MW 6 Leach 4	
Phase:	Saturation Index:
Aragonite	-1.13
Calcite	-0.98
Dolomite	-3.16
Barite	-1.76
Celestite	-3.77
Gypsum	-3.21
Strontianite	-2.83

Table 41E: Saturation indices
MW7 Leach 4

MW 7 Leach 4	
Phase:	Saturation Index:
Aragonite	-1.49
Calcite	-1.35
Dolomite	-3.37
Barite	-0.16
Celestite	-3.34
Gypsum	-3.67
Strontianite	-2.3

Table 42E: Saturation indices
MW8 Leach 4

MW 8 Leach 4	
Phase:	Saturation Index:
Aragonite	-1.84
Calcite	-1.7
Dolomite	-4.17
Barite	-0.25
Celestite	-3.49
Gypsum	-3.81
Strontianite	-2.67

Table 43E: Saturation indices
MW9 Leach 4

MW 9 Leach 4	
Phase:	Saturation Index:
Aragonite	-2.01
Calcite	-1.87
Dolomite	-4.42
Barite	-0.34
Celestite	-3.71
Gypsum	-4.04
Strontianite	-2.82

Table 44E: Saturation indices
MW10 Leach 4

MW 10 Leach 4	
Phase:	Saturation Index:
Aragonite	-1.05
Calcite	-0.91
Dolomite	-2.78
Barite	-0.17
Celestite	-3.64
Gypsum	-3.33
Strontianite	-2.5